ORO-3624-19

North Carolina State University Nuclear Structure Research at the Triangle Universities Nuclear Laboratory

Progress Report

North Carolina State University at Raleigh
Raleigh, North Carolina

Contract Period 1 April 1978 - 31 March 1979

Date of last Progress Report: 12 January 1978
Date of this Progress Report: 12 January 1979

PREPARED FOR

THE UNITED STATES DEPARTMENT OF ENERGY
UNDER CONTRACT EY-76-S-05-3624

NCSU - TUNL PERSONNEL

Faculty

Gould, C.R. (Associate Professor)
Mitchell, G.E. (Professor)
Seagondollar, L.W. (Professor)
Tilley, D.R. (Professor)
Waltner, A.W. (Professor)

Associated Faculty*

Cotanch, S.R. (Assistant Professor)
Mowat, J.R. (Assistant Professor)
Park, J.Y. (Professor)

Graduate Students

Beyerle,
Beyerle, A.
Chandler, J. (Left 6-78)
Chou, B.H.
Jensen, M.
Putcha, B. (Summer)
Sales, K.
Thambidurai, P. (Summer)
Ward, L.B.

* Not funded by Contract EY-76-S-05-3624

TABLE OF CONTENTS

INTRODUCTION

The inter-universities nature of the TRIANGLE UNIVERSITIES NUCLEAR LABORATORY and the team approaches that are necessary for experiments on large accelerators make progress reports from the three universities have a large amount of overlap.

Each year TUNL prepares an annual report which is a progress report for the entire laboratory. A report coordinator asks certain physicists to write up the work that has been done in a certain area or areas and these reports are combined. The names of the persons working in each area are listed in the report of the area.

To avoid duplication of effort and to increase accuracy, this progress report for the NCSU group (Contract EY-76-S-05-3624) is direct Xerox copy of that portion of the TUNL Annual Report XVII (1 January 1978 - 1 January 1979) in which NCSU personnel were involved. Since this portion is not all of the TUNL XVII report, appropriate changes in numbering of figures, tables and reference thereto have been made so that such numbers are sequential in this report. In each area, the names of all personnel involved are listed and the names of NCSU personnel appear underlined for easier identification.

A. NEUTRON AND FISSION PHYSICS

1. Fast Neutron Cross Sections (R.L. Walter, C.R. Gould, F.O. Purser, L.W. Seagondollar, C.E. Nelson, H.H. Hogue,* S.G. Glendinning, A. Beyerle, Sadig El Kadi, C. Floyd, E.G. Bilpuch, H.W. Newson**)

a. Experimental

(1) New Electronics Arrangement

The electronics for the neutron time of flight (TOF) detectors have been upgraded to take advantage of the superior pulse shape discrimination (PSD) capabilities of the Canberra Model 2160 NIM modules. The wide dynamic range of these units also permit operation at low bias settings without saturating the electronics for high energy recoil events.

A block diagram of the electronic setup for one of the four TOF scintillators is shown in Fig. A1-1. The anode signal from the photomultiplier

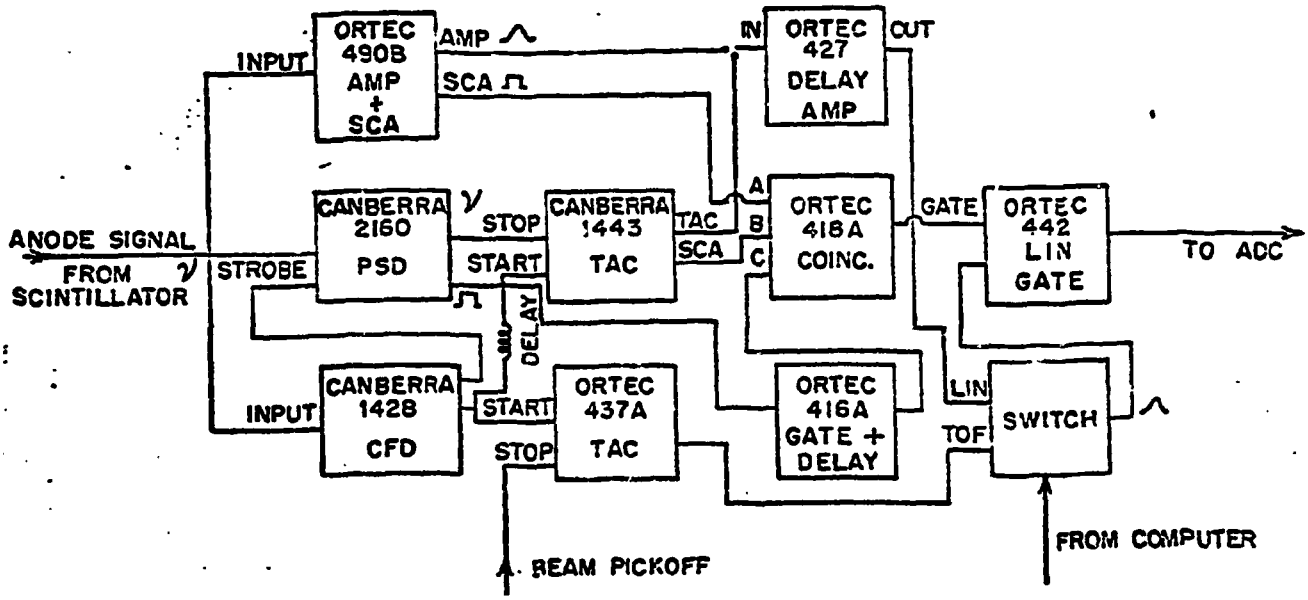

Fig. A1-1 Block diagram of electronics for TOF scintillator.

---

* Now at Oak Ridge National Laboratory

** Deceased

is used for both DSD information and linear information. The single channel analyzer (SCA) in the ORTEC 490B is used for setting the bias level for the experiment. The constant fraction discriminator (CFD) strobes the PSD unit and also provides the start signal for a Canberra 1443 time-to-amplitude converter (TAC). The stop signal comes from the PSD unit which is operated in the $n + \gamma$ mode, and the SCA output of the TAC is used to select neutron and/or gamma ray events. A separate ORTEC 437A TAC is used for the neutron TOF measurement with the stop signal coming from a capacitive beam pick off. Any of the three signals--neutron TOF, neutron PSD, or the linear neutron energy signal can be gated through to an ADC subject to the logic requirements established in the ORTEC 418A universal coincidence unit. A linear switch operated by the computer permits automatic switching between the energy and TOF signals. This switch, at the same time, activates insertion of a calibration source near the detector permitting automatic checking of the detector bias settings.

Presently four neutron detectors are operational. The two main detectors are in the heavily shielded collimators, usually at flight paths of 4m and 6m respectively for measurements of elastic and discrete inelastic scattering. For low bias continuum measurements these detectors are moved in to flight paths of ~ 3m. Two small scintillators are used to minitor the source reaction. One is at zero degrees and is used to monitor timing variations in the pulsed beam. The other detector is mounted out of the reaction plane at a flight path of 2.0 m and is used for normalizing angular distribution measurements from angle to angle.

(2) Detector Efficiency Studies

As a result of the new electronics setup and in preparation for low bias ($\leq$ 500 keV) measurements of continuum neutrons, new detector efficiency curves have been determined for the two main neutron detectors. Efficiencies for two bias settings were measured by measuring the response functions of the detectors to monoenergetic neutrons produced by the D(d,n) and T(p,n) reactions. Angular distributions were measured for incident particle energies of 6.0 MeV and 10 MeV for the D(d,n) reaction and at 2.5 MeV, 5.0 MeV and 10 MeV for the T(p,n) reaction. The overlapping data sets spanned the neutron energy range from 300 keV to 13 MeV. The energy range was extended to 16.8 MeV by measuring 0° excitation functions for the D(d,n)^{3}He reaction. All cross section data used to convert yields to efficiencies were from the compilation by Drosg[1] except for the 2.5 MeV T(p,n)^{3}He data which were taken from Liskien and Paulsen.[2] Efficiency curves for the two bias conditions are shown in Fig. A1-2.

---

[1] M. Drosg, Nuclear Science and Engineering 67, 190 (1978)
[2] H. Liskien and A. Paulsen, Nuclear Data Tables, Vol. II, no. 7, 1973

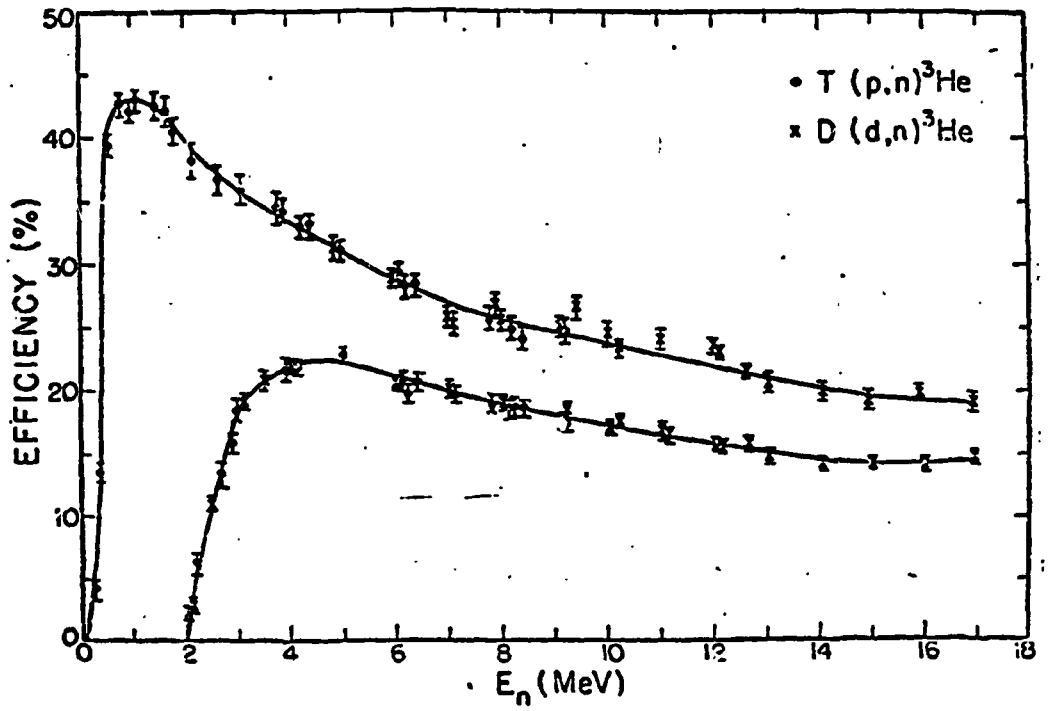

Fig. A1-2 Efficiency curves for two bias conditions.

(3) Comparison of The $D(d,n)^3He$ and $T(p,n)^3He$ Source Reactions

Both of the commonly used reactions for the production of monoenergetic neutrons have the undesirable property of also producing continuum neutrons from three-body breakup processes above the thresholds for the D(d,np)D and T(p,np)D reactions. These thresholds occur at 4.45 MeV deuteron energy and 8.35 MeV proton energy which are approximately equivalent to 7.5 MeV monoenergetic neutron energy in both cases.

For measurements of continuum neutrons from (n,xn) reactions in the presence of these "gas breakup" source neutrons, it is necessary to make four measurements to obtain the proper yields.

$$N(E_n) = [(\text{gas in, sample in}) - (\text{gas in, sample out})] - [(\text{gas out, sample in}) - (\text{gas out, sample out})]$$

where gas in and gas out refer to measurements with the target cell filled and evacuated. The spectra resulting from this subtraction process will still contain contributions from gas breakup neutrons scattered from the sample. By measuring the 0° source neutron yield simultaneously with the scattering measurements, we can make corrections for contributions from these "contaminant" neutrons in data analysis pro-

cedures. It is, however, desirable that the magnitude of this correction be kept as small as possible to minimize the computational accuracy required for the correction.

An approximate figure of merit for a neutron source reaction can be constructed by comparing its monoenergetic yield with the integral yield from three and four body breakup processes. Such a signal-to-noise ratio has been measured[1] for the D(d,n) and T(p,n) reactions for nonoenergetic neutron energies ranging from 10 to 14 MeV. Since projected neutron measurements at TUNL cover the range from 7 to 14 MeV, we undertook further tests of these reactions from 9 to 10 MeV. For neutron energies of 8.0 MeV and below, the D(d,n) reaction is the obvious selection due to its factor-of-3 additional yield.

Spectra at 0° from the D(d,n) and T(p,n) reactions for 9.2 MeV neutron energy are shown in Fig. A1-3. Gas breakup yields are integrated between the arrows indicated. In Fig. A1-4 our data for the "signal-to-noise" ratio are shown and compared to the LASL measurements. Our data agree quite well with the general trend of the previous results and it is apparent that the T(p,n) reaction retains its superiority over the D(d,n) reaction at 9.0 MeV.

(4) Electro-mechanical Changes in The NTOF Detector System

In our original time-of-flight system inherited from the Wright Patterson AFB laboratory, the massively shielded 4-meter radius detector was moved by hand from one angle to another. Even though the steel track, on which the back of the angular cart rolled, was as level as possible, moving the detector in some areas approached the physical limit of some operators. When the new 6-meter detector, which is even heavier, was installed, one operator could not move it in some areas. This problem has been solved by installation of an electric drive on each angular cart. Standing near the pivot axis where the angular position can be accurately read on a precision vernier scale, one operator now uses a push-button control which activates a high torque drive unit placed between the bottom of the angular cart and its steel track. The unit[2] is a modified "Bar, Pry, Wheeled". A 1/2-hp series-wound 110 vac motor drives, through a 315:1 ratio gear box, a pair of heavy, wide, 4" diameter rubber wheels which are in firm, adjustable contact with the steel track. The unit has a maximum rated thrust of 1900 lbs. and the angular velocity of both the 4-meter cart and the 6-meter cart is high enough that large angles can be traversed in less than a minute and yet the speed is low enough that safe operation occurs and positioning of the carts to a given angle ± 10 minutes is feasible.

---

[1] M. Drosg, et al., Los Alamos Scientific Laboratory, Internal Report LA-6459-MS (1976)

[2] These units, obtained on Federal Surplus, were manufactured for the Defense General Supply Center by Western Gear Corporation, Southwestern Division, 117 North Palmer, Houston, Texas 77003

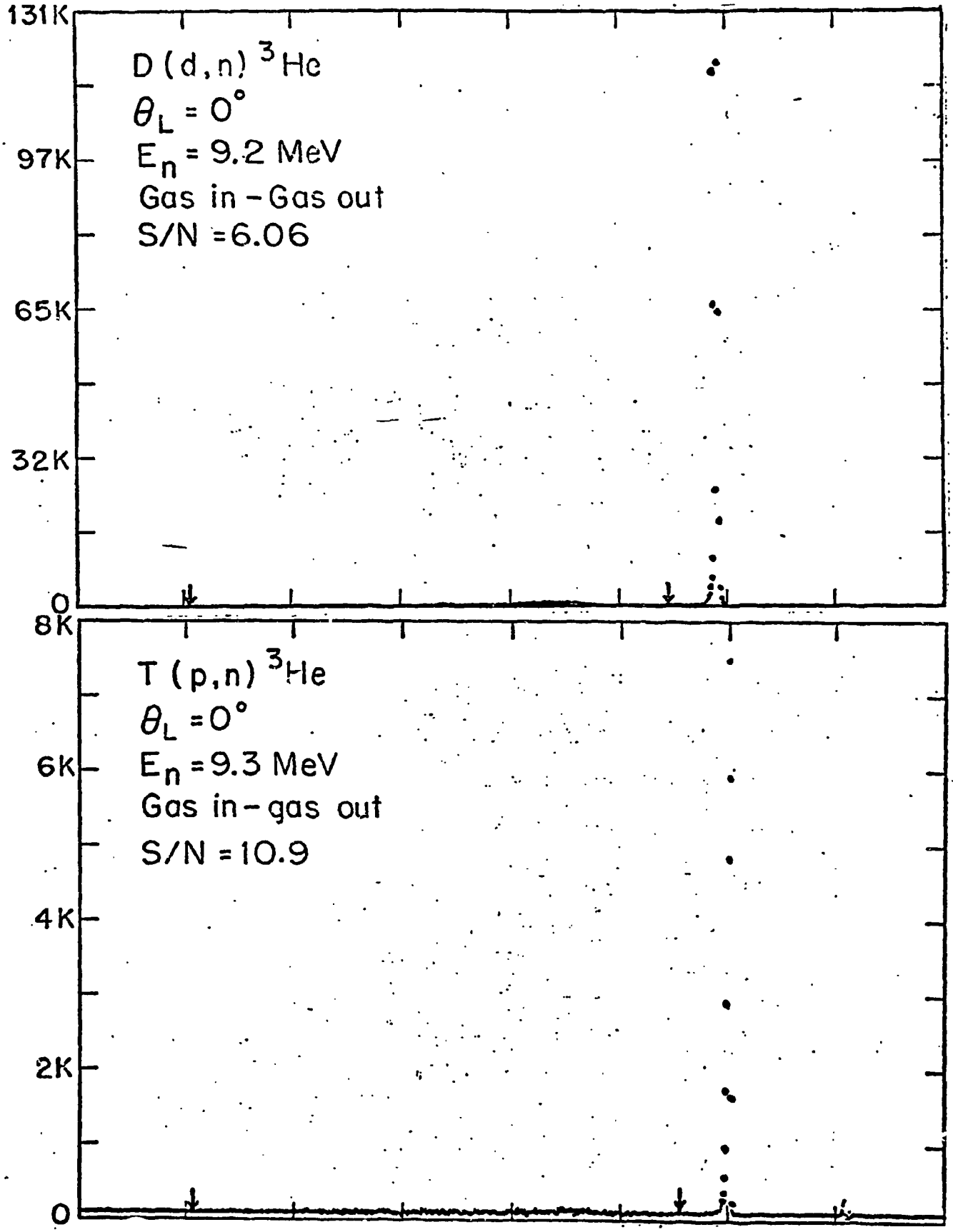

Fig. A1-3 Spectra at 0° for D(d,n) and T(p,n) reaction for 9.2 MeV neutron energy.

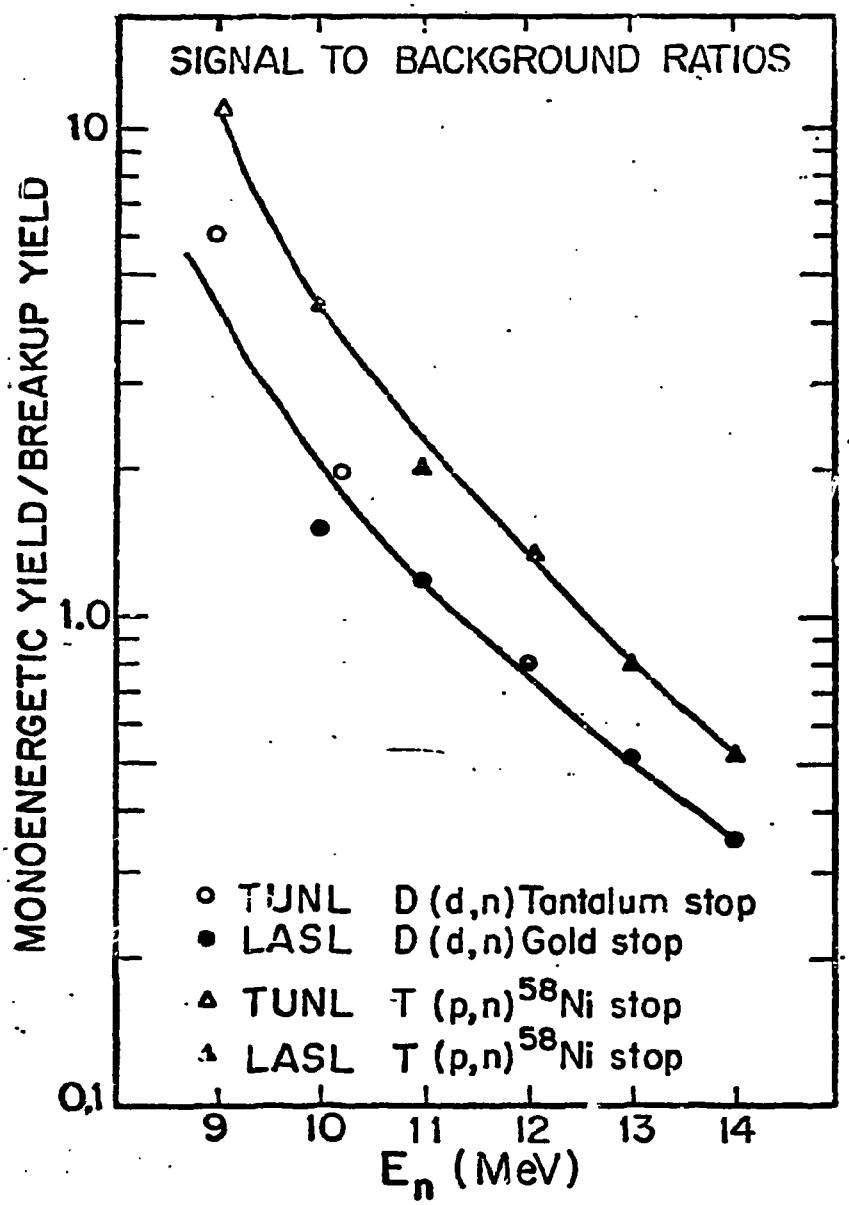

Fig. A1-4 Signal-to-noise ratio data obtained at TUNL and LASL.

Inside the shields, in both the 4-meter detector and the 6-meter detector, a lead shielded ^{241}Am source has been mounted a few inches from the liquid scintillator. By means of 180° rotation of a shaft attached to an externally mounted 72 rpm synchronous motor, the portion of the shield between the source and the scintillator is removed so the 60 keV gamma rays from the ^{241}Am can be used for bias checks. After the check, a reverse 180° rotation reshields the source. At present, these rotations are done by control room application of either -6 volt or 0 volt level signals to the relay-and-switch control of the motor. In the future, these levels will be programmed so that bias check spectra will be accumulated continuously and automatically in the computer during the time intervals between the actual time of flight runs.

In the past, our "in" scattering samples and our "out" samples had to be placed, one at a time by hand in the proper position. The horizontal location was determined by a 16-mil steel aircraft cable stretching under tension between two points which were co-axial with the pivot axis of the angular carts. A new system has been developed where five samples, six inches apart, form a portion of the cable system. The top of the cable now goes over a precisely located pulley to a one-kg weight. The bottom of the cable goes under another precisely located pulley, on to a spiral groove in a cylinder attached to the shaft of a stepping motor. The cable is fastened to the cylinder. Another cable fastened to the cylinder goes around another spiral groove and then down to a one-kg counterweight. At present, controllable frequency pulses are fed to the stepping motor until the desired sample is positioned correctly vertically as determined by the optical level. In the future, a computer program will cause the proper number of pulses to be sent to the proper winding in the stepping motor to correctly locate the desired sample automatically. The optical level will be used for any chain of five samples to determine initial positioning, operation thereafter will be computer controlled.

b. Computer Program Development for Neutron Data Correction (H. Hogue, A. Beyerle, S. El-Kadi, G. Glendinning)

Considerable work has been done during the report period on Monte Carlo data corrections programming for the neutron time-of-flight group. This activity proceeded toward three main objectives: (1) A general capability for correcting data for multi-element samples was desired. (2) An extension of the methods in use for correcting elastic and discrete inelastic scattering data to the problem of correcting continuum scattering was necessary. (3) The iterative correction procedure required reorganization to make it more straightforward, and some coding improvements were needed in preparation for publication. Two codes, dubbed EFFIGY and EFFIGYC, came about as a result of the work.

Program EFFIGY is a reorganized version of program MC, described in a previous report. Its purpose is to calculate attenuation, finite geometry, and multiple scattering effects for cylindrical samples of one or more elements. In process of obtaining these corrections, differential cross section libraries are input and time-of-flight spectra, analogous to the experimental spectra, are

calculated and summed over the time windows used in the experiment. A facility for subtracting previously calculated "out-count" spectra from the calculated spectra before window summation has been included. Thus, secondary effects of truncation of the timing tails in summing experimental spectra and over- or under-subtraction of the "out-count" spectra are corrected.

Program EFFIGYC is a companion program for EFFIGY, using most of the same subroutines but designed to correct "continuum" scattering data. The program takes as input differential cross section libraries for scattering to states at excitations low enough to give distinct groups in the time-of-flight spectra. It thus determines the energy distribution resulting from all other scattering processes, which (after correction for attenuation, finite geometry, and multiple scattering effects), gives the observed time-of-flight spectra. The removal from the scattering spectra of scattered gas breakup neutrons from the target cell has also been included in EFFIGYC.

c. CTR Related Measurements

(1) Lithium 6 and Lithium 7

A paper reporting the results of this measurement has been accepted for publication in Nuclear Science and Engineering.

(2) Boron 10

Eight angular distributions of elastic and inelastic scattering have been measured for incident neutron energies from 8.0 to 14.0 MeV. At the higher energies inelastic scattering to the 0.717 MeV state was not resolved from the elastic group.

Data were taken with a 92.41% enriched ^{10}B sample. Corrections for the 7.59% admixture of ^{11}B will be incorporated in the data analysis using our two-element Monte Carlo code and a combination of the ^{11}B ENDF4 library and ^{11}B elastic and inelastic cross sections previously measured at TUNL. The data is in the analysis stage.

(3) Boron 11

Eight angular distributions for elastic scattering and for inelastic scattering resulting from the 2.14, 4.46 and 5.04 MeV states have been measured for incident neutron energies from 8.0 to 14.0 MeV. Analysis has been completed on these data which will be transmitted to NNDC as a package with the ^{11}B data.

(4) Oxygen 16

Internal consistency checks prior to final release revealed discrepancies in three of the angular distributions for this isotope reported previously.

All of the data in question were acquired during a single experimental run. These angular distributions at 10.75, 11.5 and 12.5 MeV have been remeasured and the entire data set recorrected for finite size and multiple scattering effects using our improved Monte Carlo code EFFIGY. They are again in the process of final formatting for release to NNDC. The revised data are shown in Figure A1-5.

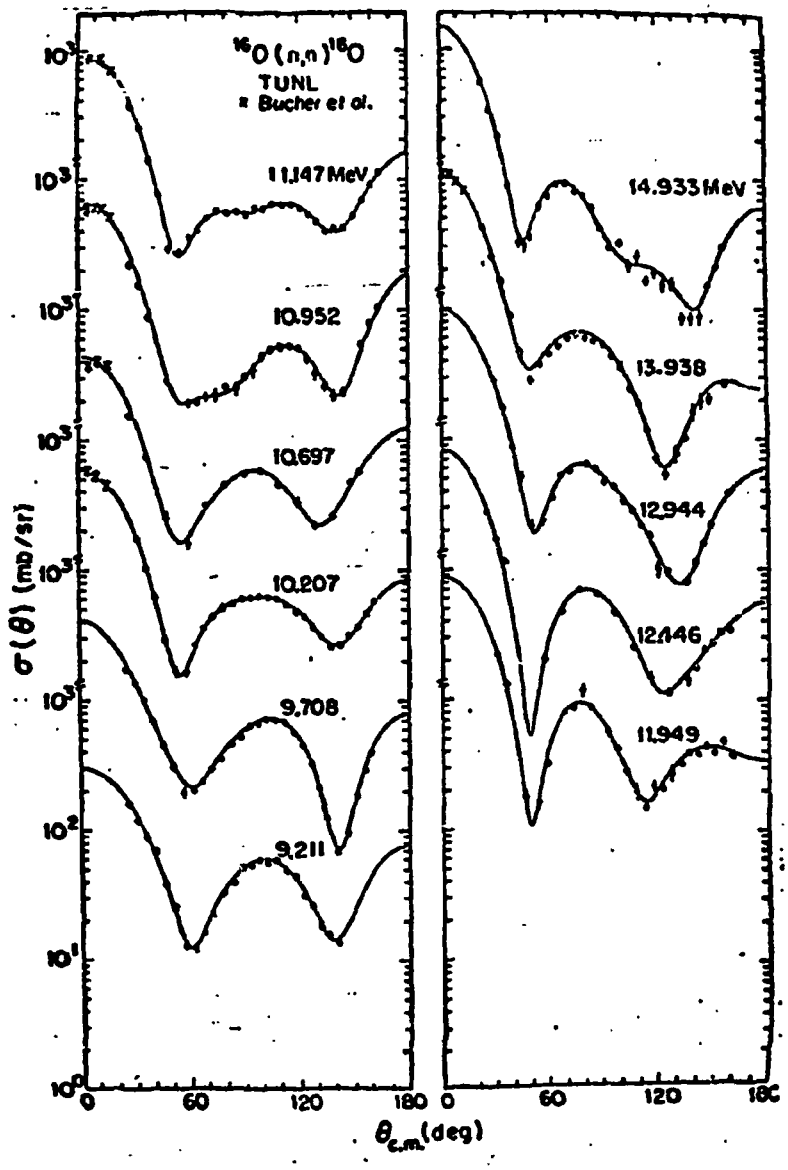

Fig. A1-5 Differential cross sections for $^{16}O(n,n)^{16}O$.

(5) ^{54}Fe and ^{56}Fe

Neutron scattering measurements with isotopic samples of ^{54}Fe and ^{56}Fe are presently underway. Two types of measurement are being made:

i) Elastic and first excited state inelastic scattering angular distributions at angles from 30 to 155 in 5° increments using the D(d,n) source reaction.

ii) Continuum neutron spectrum studies at a few angles with the T(p,n) source reaction.

For the elastic scattering angular distributions the maximum flight paths of 4m and 6m are employed for the detectors, and data have been obtained at 10 and 12 MeV bombarding energy. For the continuum measurements we are primarily interested in the lower energy neutrons and reduced flight paths of 2.7 and 3.7 m are employed. The detectors are biased at ~300 keV equivalent neutron energy and the T(p,n) source reaction is used because of the reduced background of breakup neutrons from the gas compared to the D(d,n) reaction. Low bias measurements have been made at 40°, 80°, 125° and 160° at 5.9 MeV; 35°, 65°, 95°, 125° and 155° at 9.1 MeV; and 80° and 125° at 10.1 MeV. Fig. A1-6 shows a difference time-of-flight spectrum obtained at 40° and 5.9 MeV bombarding energy with a flight path of 3.7 m. Here four spectra (gas in, sample in; gas in, sample out; gas out, sample in; gas out, sample out) have been normalized and subtracted to obtain the final $^{56}Fe(n,n')$ time-of-flight spectrum. At this energy, 11 discrete inelastic scattering groups are seen in the spectrum down to ~700 keV neutron energy. Analysis of the data is proceeding.

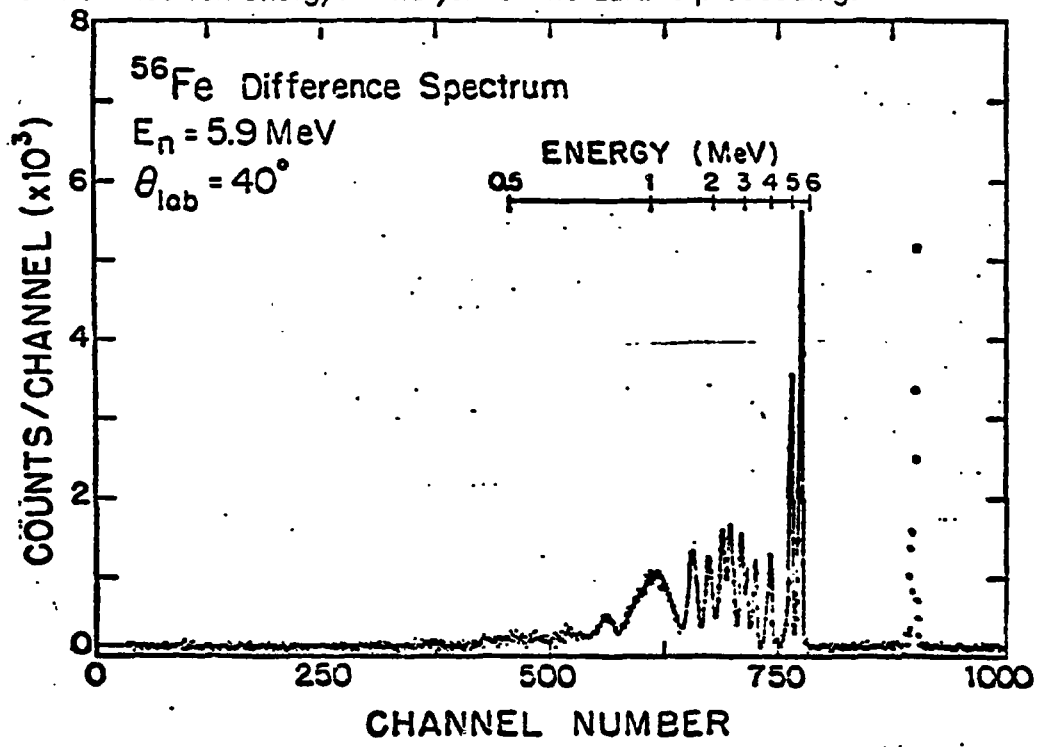

Fig. A1-6 A difference time-of-flight spectra for ^{56}Fe + n.

B. HIGH RESOLUTION STUDIES

1. High Resolution Elastic Scattering (E.G. Bilpuch, G.E. Mitchell, M.E. Bleck,* K.B. Sales, W.A. Watson, W.K. Wells,** C.R. Westerfeldt, K.M. Whatley)

The primary interests in elastic scattering concern the proton strength function and highly fragmented analogues. To obtain more information on the proton strength function we have extended our measurements on both the low mass end (^{26}Mg) and the high mass end (Zn). Our analogue state emphasis has been on ^{90}Zr.

a. ^{26}Mg

A paper has been published on this work: "High Resolution Study of the ^{26}Mg(p,p) Reaction", C.R. Westerfeldt, G.E. Mitchell, E.G. Bilpuch, and D.A. Outlaw, Nucl. Phys. A303, 111 (1978). The following is the abstract of that paper:

> "The differential cross section for ^{26}Mg(p,p) was measured from E_p = 1.54 to 3.06 MeV at lab angles of 90°, 105°, 135° and 160° with an overall energy resolution of ≈400 eV. Resonance parameters were determined for 61 resonances. Strong analogues of the sixth ($1/2^+$), eigth ($3/2^-$) and ninth ($7/2^-$) excited states of ^{27}Mg were identified and tentative identifications suggested for analogues of the seventh ($3/2^+$) and tenth ($3/2^+$) excited states. Spectroscopic factors and Coulomb energies were determined. One striking shift in the Coulomb energies was observed: the analogue of the eigth excited state of ^{27}Mg occurs below the analogues of the sixth and seventh excited states. The present values for Γ_p were combined with the results of previous capture measurements and total γ-ray widths determined for almost all of the resonances observed below E_p = 2.6 MeV."

These data also provide a showcase example of the success of the multilevel fitting procedure. In Fig. B1-1 is shown data and fit in an energy region with resonances of $J^\pi = 1/2^+, 1/2^-, 3/2^-, 3/2^+, 5/2^+, 5/2^-, 7/2^-$ and with widths ranging from 10 eV to 30,000 eV.

---

* Now at Sandia Laboratories

** Now at University of Pennsylvania

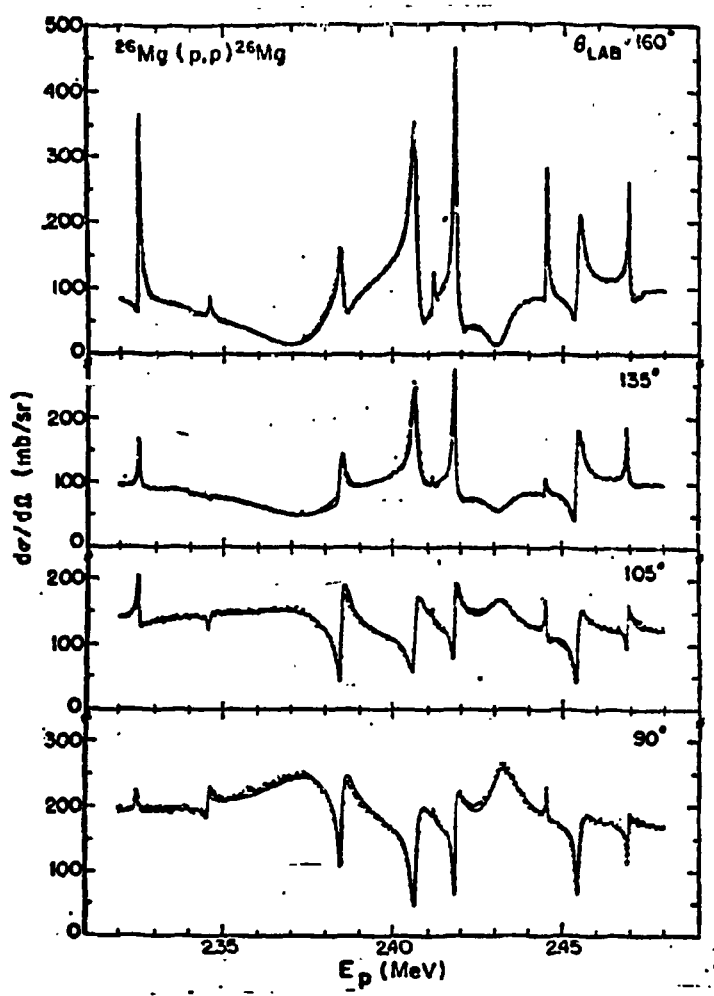

Fig. B1-1 The $^{26}Mg(p,p)^{26}Mg$ differential cross section from E_p = 2.32 to 2.48 MeV at four angles. The solid line is the multi-level R-Matrix fit to the data.

b. Zn

Our efforts on the Zn isotopes are primarily to obtain information concerning the s-wave strength function. This work has been delayed by difficulties in preparing Zn targets suitable for high resolution measurements. We have fabricated a glow-discharge system for preparing Zn targets, and expect to have more suitable targets in the near future. We then plan to study ^{66}Zn. Meanwhile, we have measured elastic scattering from ^{64}Zn from E_p = 2.50 to 3.24 MeV. Although the quality of the data is not as high as we would like, the data have been analyzed and the essential features of the results obtained. The s-wave strength function is $s_0 = 0.05$, consistent with all of our previous results and showing no sign of the 3s size resonance. In addition spectroscopic properties of three analogues ($1/2^-$, $3/2^-$ and $5/2^+$) were obtained. A preliminary report on this work was given at the Southeastern Section of the American Physical Society, October, 1978.

c. ^{90}Zr

The lowest s-wave analog state in ^{91}Nb was studied extensively with the FN tandem accelerator. Although the level density is so great that the fine structure was incompletely resolved, valuable information about both the experimental system and highly fragmented analog was obtained. The following is the abstract of a dissertation by M.E. Bleck:

> "Excitation functions for the reaction $^{90}Zr(p,p)$ were measured from 5.684 to 5.992 MeV at laboratory angles of 90°, 107°, 135° and 160°. Proton energy resolution varied between 425 and 450 eV. The data were fit to an R-matrix cross section containing 302 s-wave resonances. These levels comprise the fine structure of the lowest $1/2^+$ analogue state in ^{91}Nb.
>
> Excellent beam energy resolution was maintained through use of a three loop energy regulating system adapted for high resolution work at TUNL specifically for this experiment. This system includes an optical feedback path which permits high voltage modulation of the terminal stripper in order to null residual energy fluctuations.
>
> The fine structure distribution was incompletely resolved due to the extremely high compound nuclear level density. Nevertheless, a good fit to the theoretical distribution (Lane 1969) was obtained. The fine structure parameters extracted from the fit were found to be in mild disagreement with those obtained in an earlier, thick target experiment (Richard et al., 1971). Severe disagreement between the Robson estimate and the experimental value was obtained for the analogue spreading width.
>
> The statistical distributions of resonance widths and spacings were examined as a check on the R-matrix fitting procedure.
>
> The analogue proton spectroscopic factor was deduced and compared with spectroscopic factors for the parent and anti-analogue states obtained from the literature."

2. High Resolution Inelastic Scattering (G.E. Mitchell, E.G. Bilpuch, J.R. Chandler,* B.H. Chou, W.A. Watson, W.K. Wells,** C.R. Westerfeldt)

The program of high resolution inelastic scattering has developed rapidly during the past year. These measurements of magnitudes and relative phases (signs) of inelastic amplitudes provide a variety of new and interesting results for both doorway (analog) states and for statistical properties of widths. These multichannel studies of analog states provide subtle ways to test analog state theory, as well as more sensitive tests for non-statistical effects. The critical point is that the theories are formulated in terms of width amplitudes γ, but normal experiments measure the reduced widths γ^2. Since the measurement of amplitudes themselves are impossible, the best one can do is measure magnitudes and relative signs in multichannel processes.

The method involving inelastic scattering is very simple. Consider for isolated resonances the reaction $A(p,p')B^*$ followed by $B^* \rightarrow B+\gamma$. For our case $A= B= 0^+$, $B^* = 2^+$. For p-wave resonances, the p' and γ-ray angular distributions are both isotropic for $1/2^-$ resonances, but cannot be simultaneously isotropic for $3/2^-$ resonances. Thus we can uniquely distinguish between $1/2^-$ and $3/2^-$ resonances. If one can neglect $\ell' = 3$, then there are only 2 inelastic amplitudes ($j' = 1/2$ and $j' = 3/2$). The p' and γ-ray angular distributions suffice to determine the magnitudes $\gamma_{1/2}$, $\gamma_{3/2}$ and the sign of $\gamma_{1/2}\gamma_{3/2}$. Rephrased, the experiment determines the mixing ratio $\delta_j = \gamma_{3/2}/\gamma_{1/2}$. As in the electromagnetic case, it is often convenient to convert to $\phi = \tan^{-1}\delta$. Although similar measurements have been performed for isolated resonances, and for a very few cases the value δ_j was determined for a number of resonances, these are the first measurements of both the magnitude and sign of δ for many resonances.

We have generalized these results by extending the analysis to $d_{3/2}$, $d_{5/2}$, $f_{5/2}$, $f_{7/2}$, $g_{7/2}$, $g_{9/2}$ resonances and have also removed the restriction to one exit ℓ' value. For $p_{1/2}$ and $p_{3/2}$ states, the former can decay to a 2+ state only by $j' = 3/2$, while the latter can decay by $j = 1/2$ and $3/2$. Thus, a $p_{1/2}$ resonance has a unique angular distribution, while a $p_{3/2}$ resonance has channel spin mixing. Except for d-wave resonances, this pattern carries through for other resonances--$f_{5/2}$ and $g_{7/2}$ states show mixing, while $f_{7/2}$ and $g_{9/2}$ resonances have unique distributions. Admixtures of higher ℓ'-values are expected to be small due to low penetrabilities, but must be included in general. A useful notation is

$$\delta(\text{lower}) = \frac{<(\ell'_{\text{lower}} + 1/2)>}{<(\ell'_{\text{lower}} - 1/2)>} \quad , \quad \delta(\text{higher}) = \frac{<\ell'_{\text{higher}} + 1/2>}{<\ell'_{\text{higher}} - 1/2>} \quad \text{and}$$

$\epsilon^2 \equiv (\ell_{\text{higher}}\ \text{strength})/(\text{total strength})$. The d-wave resonances are special. Since the lowest possible ℓ' value is $\ell' = 0$, there is no δ(lower), but δ(higher) and ϵ^2 can still be measured. In practice we have now measured many p-wave resonances, a number of d-wave resonances, a dozen f-wave resonances and one $g_{9/2}$ resonance.

---

* Now at Savannah River

** Now at University of Pennsylvania

The thrust of this work was summarized recently in an invited talk at the 1978 Small Accelerator Conference: "High Resolution Proton Scattering", G.E. Mitchell, Bull. Am. Phys. Soc. 23, 1023 (1978). The following is the abstract of that talk:

> "Results from the high resolution proton resonance studies at TUNL are presented. The thousands of resonances analyzed provide a body of data unique in charged particle resonance spectroscopy, with significant results in both statistical and non-statistical areas. One major area which has been explored in depth is the fine structure of analogue states. In another major area, detailed statistical analysis of spacing distributions confirm the existence of both short and long range correlations among level spacings. In addition to continuing work in these and related areas, recent emphasis has been placed on new experimental methods which permit the measurement of correlations between amplitudes in different channels. These results confirm predictions for common doorways, provide sensitive probes to search for non-statistical effects, and permit more detailed tests of certain statistical assumptions than hitherto possible. The experimental method for these latter measurements is described, and new data presented."

a. Off-Diagonal Strength Function

The reduced widths in these channels for an analog in ^{45}Sc are shown in Fig. B2-1, along with the product of the inelastic reduced width amplitudes.

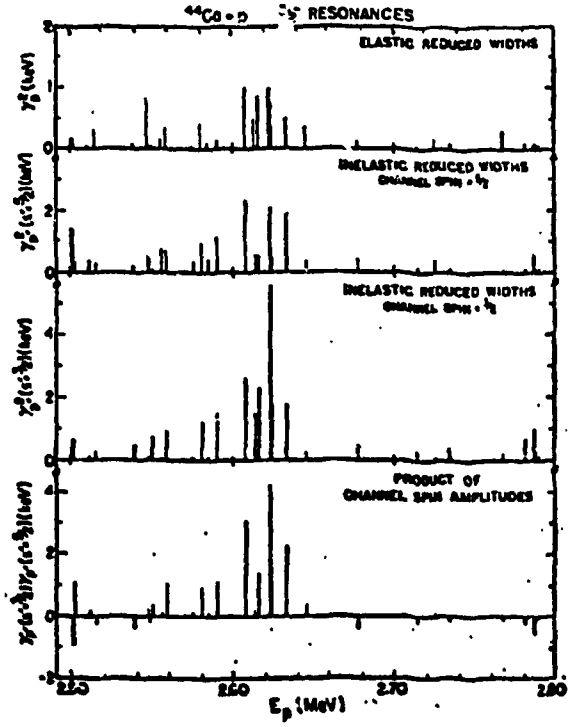

Fig. B2-1 (a) – (d). Plots of reduced width quantities $\gamma_{\nu o}^2$, $\gamma_{\nu 3}^2$, $\gamma_{\nu 5}^2$, $\gamma_{\nu 3}\gamma_{\nu 5}$ versus the energy of the $3/2^-$ resonances ν. $\gamma_{\nu o}^2$ are the widths of the elastic channel ^{44}Ca + p, while $\gamma_{\nu 3}^2$, $\gamma_{\nu 5}^2$ refer to channel spins $s' = 3/2, 5/2$ in the inelastic channel with ^{44}Ca in the 2^+ state at 1.57 MeV.

Standard theory gives for the form of $s_{cc'}$ near an analogue λ

$$s_{cc'} = A_{cc'} + \frac{1}{\pi} \text{Im.} \frac{\alpha_{\lambda c}\, \alpha_{\lambda c'}}{E_\lambda - E - (i/2)W_\lambda}$$

where $A_{cc'}$ is the "background" strength-function, E_λ and W_λ are the energy and width of the analogue, and $\alpha_{\lambda c}$ is the (complex) reduced width amplitude of the analogue in channel c. This may be rewritten:

$$s_{cc'} = A_{cc'} + \frac{B_{cc'}(E_\lambda - E) + C_{cc'}}{(E_\lambda - E)^2 + W_\lambda^2/4}$$

where:

$$\frac{2C_{cc'}}{W_\lambda} + iB_{cc'} = \frac{1}{\pi} \alpha_{\lambda c} \alpha_{\lambda c'}$$

The implication of this equation is that, apart from a sign, the diagonal quantities B_{cc}, C_{cc}, $B_{c'c'}$, $C_{c'c'}$ imply values of the off-diagonal quantities $B_{cc'}$, $C_{cc'}$:

$$(C_{cc'} + \frac{i}{2} W_\lambda B_{cc'})^2 = (C_{cc} + \frac{i}{2} W_\lambda B_{cc})\,(C_{c'c'} + \frac{i}{2} W_\lambda B_{c'c'})$$

Thus, given the diagonal strength-functions, s_{cc} and $s_{c'c'}$, we may predict the energy-dependent part of the off-diagonal strength-function $s_{cc'}$. From fitting the diagonal data of Fig. B2-1 we obtain the values: $B_{33} = 1.82$, $C_{33} = 57.3$, $B_{55} = 1.32$, $C_{55} = 29.8$, where B,C values are in (keV), $(\text{keV})^2$, and the subscripts are twice the exit channel spin. This gives $B_{35} = 1.71$, $C_{35} = 41.4$ or $B_{35} = -1.71$, $C_{35} = -41.4$. The diagonal fits also give $E_\lambda = 2.624$ MeV, $W_\lambda = 15$ keV. In Fig. B2-2, we compare the predictions of s_{35} arising from both the positive choice of B_{35}, C_{35} (solid curve) and the negative choice of B_{35}, C_{35} (dashed curve) with the data. To remove fluctuations,

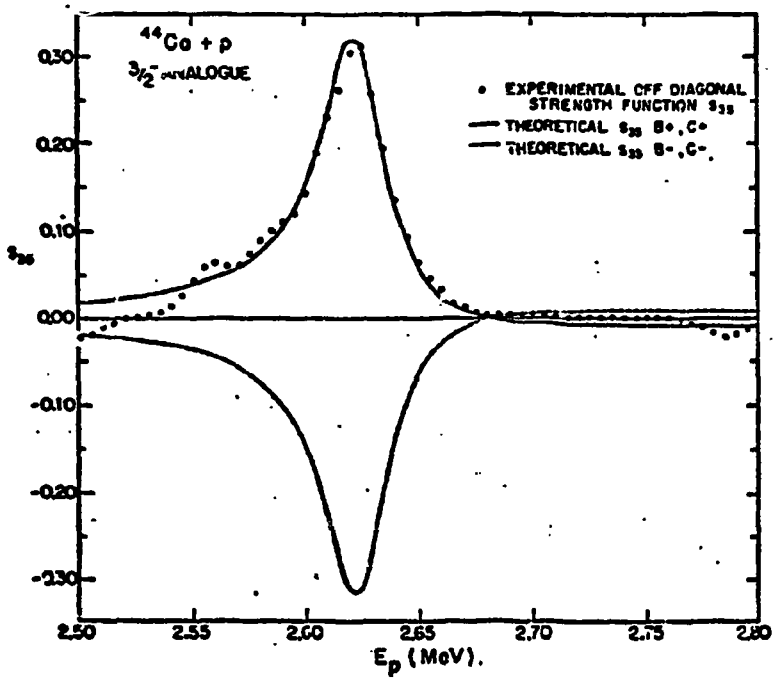

Fig. B2-2 Comparison of experiment and theory for the off-diagonal strength function s_{35}. (see text).

both quantities have been averaged over energy with a Lorentzian envelope of width 20 keV. The fit for the positive values of B_{35} and C_{35} is good.

This work was reported in a recent paper "New Probe of Line Broadening with Resolvable Fine Structure: The Off-Diagonal Strength Function", A.M. Lane, T.R. Dittrich, G.E. Mitchell, and E.G. Bilpuch, Phys. Rev. Letters 41, 454 (1978).

b. ^{44}Ca

Several papers have been published on our experimental results on $^{44}Ca(p,p'\gamma)$ in the vicinity of the analog resonance at $E_p = 2.62$ MeV. One Phys. Rev. Letters article on the off-diagonal strength function was described in the previous section. Another paper was presented at the "Third International Symposium of Neutron Capture Gamma-Ray Spectroscopy and Related Topics": "Experimental Demonstration of Phase Relation for Common-Doorway States", G.E. Mitchell, T.R. Dittrich, and E.G. Bilpuch. A more detailed paper has been accepted for publication by Zeitschrift für Physik: "Study of Inelastic Proton Amplitudes for a Fragmented Analog State in ^{45}Sc", G.E. Mitchell, T.R. Dittrich, and E.G. Bilpuch. The following is the abstract of that paper:

> "The relative sign of inelastic proton-channel amplitudes has been measured for 31 resonances in ^{45}Sc. These resonances include the fragmented $3/2^-$ analog state observed at $E_p = 2.62$ MeV in the $^{44}Ca(p,p)$ and $^{44}Ca(p,p')$ reactions. The analog fine structure is analyzed for the elastic and two inelastic channels; the Robson asymmetry is displayed clearly in the inelastic channels. The relative sign of the mixing ratio remains the same for the 15 fine structure resonances of the analogue. The mixing ratios enable the determination of the amplitude correlation of the widths in the inelastic channels. The recently introduced "off-diagonal strength function" is constructed from these data and compared with the theory of analog state broadening."

c. ^{46}Ti

Results on the $^{46}Ti(p,p')$ reaction provided another example of the constancy of the relative sign for amplitudes in a common doorway. The following is the abstract of the dissertation of John R. Chandler:

> "The $^{46}Ti(p,p'\gamma)^{46}Ti$ reaction was investigated between the proton bombarding energies 2.25 and 3.10 MeV using the high resolution system of the Triangle Universities Nuclear Laboratory 3 MV Van de Graaff accelerator. Both the proton and the de-

excitation gamma-ray angular distributions were measured for thirty-four p-wave and f-wave resonances. Expressions for the angular distributions are given for the inelastically scattered protons and for the de-excitation gamma-rays in two angular momentum coupling schemes for p-wave and f-wave resonances. Simple expressions are also derived for transformations between the two representations. The results of the two singles measurements unambiguously determine the spin of the compound state for each resonance, and the magnitudes and the relative sign between the inelastic amplitudes are obtained. In general the experimental results in the analogue state regions are nonstatistical. The off-analog data also suggest possible nonstatistical effects. In addition, properties of the observed analog states are obtained with emphasis on the fine structure of the analogue at $E_p = 2.87$ MeV."

A paper on these results will be prepared in the near future.

d. ^{48}Ti, ^{56}Fe

A large number of p-wave resonances have been investigated in ^{49}V and ^{57}Co. The $^{48}Ti(p,p'\gamma)$ data are particularly extensive and interesting. Analysis of these results is continuing. The following is the dissertation of W.K. Wells:

"Inelastic proton decay from p-wave resonances in ^{49}V and ^{47}Co were studied using the high resolution proton beam from the Triangle Universities Nuclear Laboratory's 3 MV Van de Graaff accelerator. The inelastically scattered proton and de-excitation gamma-ray angular distributions were measured at four angles for one hundred and twenty resonances in ^{49}V and thirty-six resonances in ^{57}Co. The results of the two singles measurements unambiguously determine the spin of the compound nuclear state for each resonance. The magnitudes and relative phase of the two inelastic decay channel amplitudes were measured for $3/2^-$ resonances.

Inelastic spectroscopic factors were determined for three isobaric analog states in ^{57}Co and for two isobaric analog states in ^{49}V. The strength functions for the elastic and inelastic scattering channels were calculated from the average spacing and reduced width data.

A sequence of 72 $3/2^-$ resonances in ^{49}V was used to test the statistical hypotheses for width distributions

in the orthogonal ensemble. Evidence is presented for non-statistical behavior indicative of two doorway states in ^{49}V."

e. ^{54}Fe

Angular distributions have been measured for ten f-wave resonances and 1 $g_{9/2}$ resonance in the $^{54}Fe(p,p'\gamma)$ reaction. Five of the f-wave resonances and the g-wave resonances were previously identified as analog states. All of the f resonances have $j = 5/2$. Contrary to previously published claims, the analog at $E_p = 3.80$ MeV has a very small $\ell' = 3$ component--only about 1%. The data are consistent with the $j = 9/2$ assignment for the g-state. A preliminary report on these data has been presented at the Southeastern Section Meeting of the American Physical Society, October, 1978.

f. ^{45}Ti - d-wave Resonances

Since $\ell = 0, 1, 2$ resonances predominate in the 1f-2p shell, and since $\ell = 0$ resonances are not suitable for these inelastic measurements, our emphasis is on p- and d-wave resonances. Our first study on d-wave resonances is the $^{48}Ti(p,p'\gamma)$ reaction. There are no $\ell = 2$ analogs in the region under study. We have studied 70 resonances in the energy region $E_p = 2.7 - 3.1$ MeV. Empirically the $\ell = 2$ admixture appears to be large enough to study and the data enable a distinction between $d_{3/2}$ and $d_{5/2}$ resonances. Analysis of these data is in progress.

C. GAMMA RAY SPECTROSCOPY

1. Spin Assignment of The 11.86 MeV Level in ^{24}Mg (S.A. Wender, C.R. Gould, D.R. Tilley, D.G. Rickel, R.W. Zurmühle ((Univ. of Pennsylvania)))

This work has been published in Physical Review C17 (1978) 1365. The abstract follows:

"Linear polarizations of γ rays from the 11.86 → 8.12 → 4.12 MeV decay in ^{24}Mg have been studied with a NaI polarimeter. The 11.86 MeV level was populated via the $^{12}C(^{16}O,\alpha\gamma)^{24}Mg$ reaction. The results are consistent with $J^\pi = 8^+$ for the 11.86 MeV level and in agreement with earlier work, rule against a 6^+ assignment with 85% confidence."

D. RADIATIVE CAPTURE REACTIONS

1. The Capture Program - General Status (N.R. Roberson, H.R. Weller, S.A. Wender, D.R. Tilley, M. Jensen, S. Manglos, L. Ward, M. Wright, C. Fitzpatrick)

The basic experimental set-up for radiative capture measurements remains the same as described in the previous report. The arrangement is shown in Fig. D1-1 below.

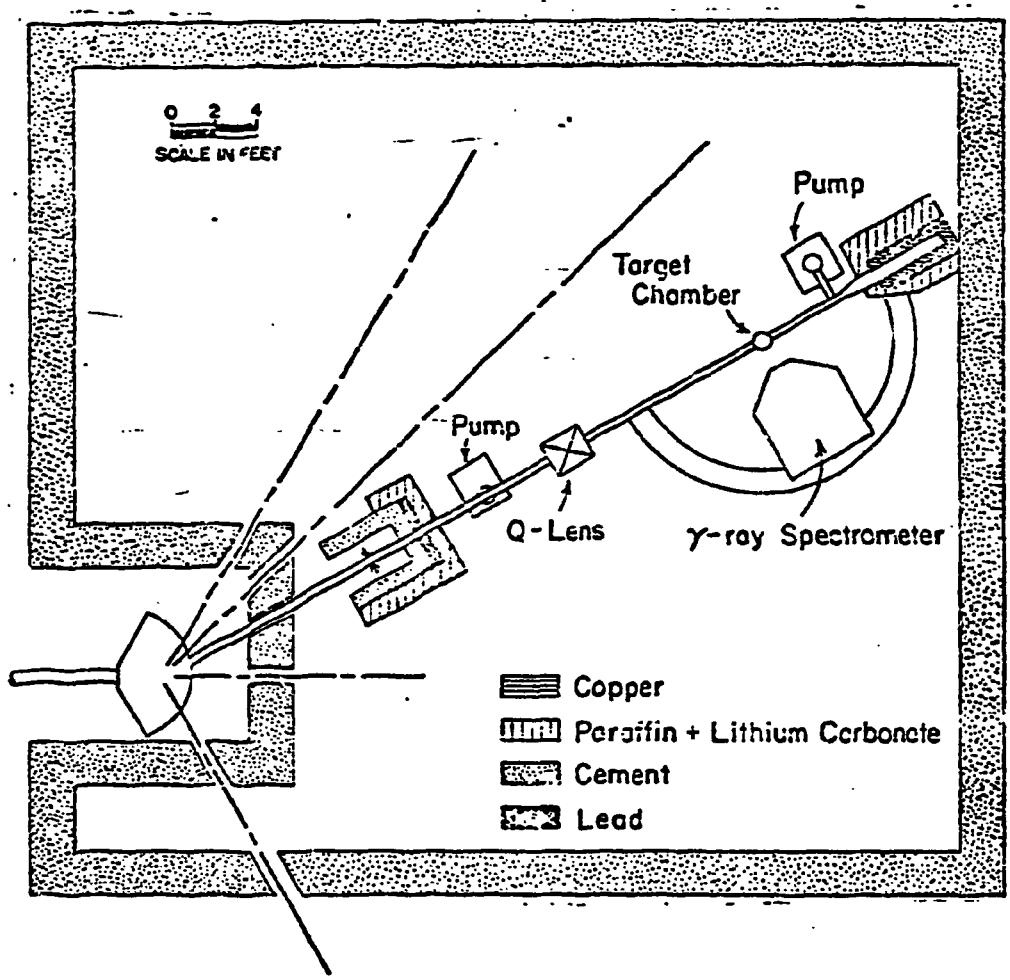

Fig. D1-1. Physical arrangement of the gamma-ray spectrometer in the target room.

A considerable effort has been made to document the spectrometer's efficiency--especially the energy dependent effects (e.g., attenuation and rejection effects). For our neutron capture studies we have been working to improve the shielding and reduce the background in general. We have found some improvement by increasing the deuterium gas cell pressure from 2 to 3 atmospheres, with a corresponding reduction in the beam intensity. Other changes, such as removing the beam dump material and the copper shielding which has been placed in front of the detector to attenuate high energy neutrons, appear to reduce the background count rate in the detector by about a factor of four. Our acquired experience with the positioning of the shadow bar has also made for more reliable results. In addition we have improved our neutron flux monitoring with the installation of a collimated zero degree monitor. A proton recoil counter has also been built and used to check our flux calibration.

The main emphasis of our capture program continues to be centered around the search for effects of the giant quadrupole resonances. The experiments involving polarized proton capture have been extensively analyzed by means of the direct-semidirect reaction theory. Our principle conclusions are:

1. A simple DSD model calculation of the E1 relative amplitudes and phases accounts for the general features observed in the experiment. Furthermore, this calculation provides a reliable means for choosing one of the two possible E1 solutions which are usually obtained from the experimental data.

2. Most of the E2 effects which we have been able to observe in proton capture are consistent with a calculation which assumes only direct E2 radiation. So it appears that this "background" E2 strength, along with the apparent weak strength of the isoscalar E2 resonance in the ground state proton channel, makes for an unfavorable situation vis a vis a study of the E2 isoscalar resonance.

3. The proton capture fore-aft asymmetry measurements which we have made in the energy region expected to contain the isovector E2 resonance have been carefully analyzed using the direct semidirect theory. These results are very encouraging and provide convincing evidence for a positive result in the case of $^{30}Si(p,\gamma_1)^{31}P$. Since the cyclotron is again operational, and since the direct semidirect theory seems to provide an effective tool for analyzing asymmetry data, we expect to begin a serious effort to investigate 20-30 MeV proton capture--especially directed towards observing the effects of the isovector GQR. This program should get underway this winter.

4. The neutron capture reaction appears to be a more favorable tool for studying the E2 resonances. This is primarily a result of the fact that the direct E2 strength is virtually eliminated as a result of the small quadrupole effective charge of the neutron. We have found that we observe a finite fore-aft asymmetry in the case of n capture by ^{40}Ca, which can be accounted for by including the (previously observed)[1] isoscalar E2 resonance in a direct-semidirect model calculation.

5. We have found that polarized neutron capture appears to be quite sensitive to non E1 radiation. Although we have just begun to perform these measurements, our results for the case of $^{40}Ca(\vec{n},\gamma)$ display rather large b_1 coefficients. Indeed the effects are much larger than the fore-aft asymmetry effects previously mentioned (typically 20% vs 5% effects). A detailed comparison with the predictions of the DSD theory is underway. It appears that these measurements may provide a viable technique for studying the giant quadrupole resonances. They will certainly provide a more stringent test of the DSD theory.

6. Our initial effort using polarized capture in the case of a few nucleon problem involved the $D(\vec{p},\gamma)^3He$ reaction (to be published). The results in this case were quite interesting. Recent continuum shell model calculations[2] have indicated that the analyzing power observed in certain few nucleon capture problems is related to the spin-orbit odd component of the effective nuclear force. This, plus our ability to measure both polarized neutron and polarized proton capture, suggests that we should perform experiments such as $^3He(\vec{n},\gamma)^4He$ and perhaps $D(\vec{n},\gamma)T$. Such experiments are being planned for the near future.

---

[1] D.H. Youngblood, J.M. Moss, C.M. Rozsa, J.D. Branson, A.D. Becker and D.R. Brown, Phys. Rev. C13, 994 (1976)

[2] D. Halderson and J. Philpott, Private Communication

2. The $^{13}C(\vec{p},\gamma_{0,1})^{14}N$ Reaction (J.D. Turner, N.R. Roberson, S.A. Wender, S.H. Manglos, H.R. Weller, M.J. Jensen, D.R. Tilley)

The 90 degree yield curves for the $^{13}C(p,\gamma_0)^{14}N$ and $^{13}C(p,\gamma_1)^{14}N$ reactions have been measured in 200 keV steps for incident proton energies of 6.25 to 13.6 MeV and in 100 keV steps for E_p of 13.6 to 17.0 MeV. In addition, data were obtained at proton energies from 12.6 to 14.55 MeV in 50 keV steps. These data are shown in Figs. D2-1 and D2-2. The integrated yield for the ground state transi-

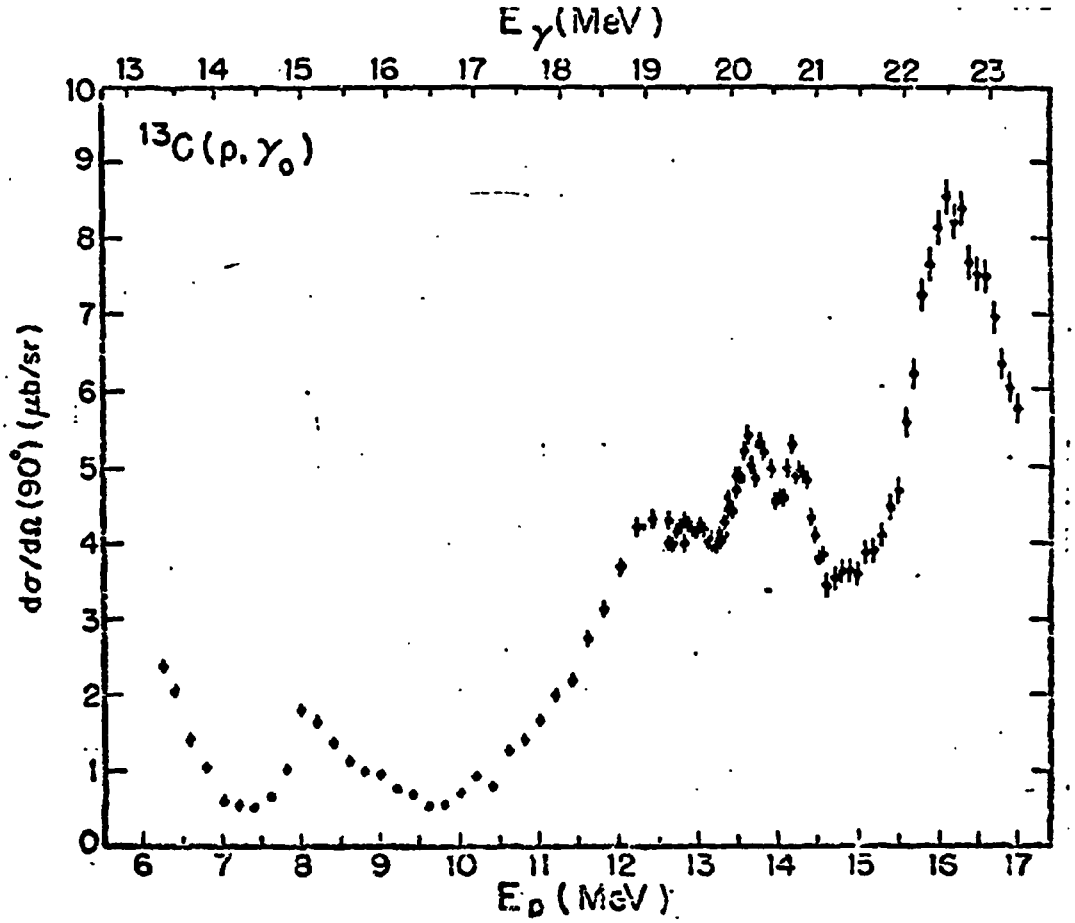

Fig. D2-1 The 90° yield curve obtained for the $^{13}C(p,\gamma_0)^{14}N$ reaction.

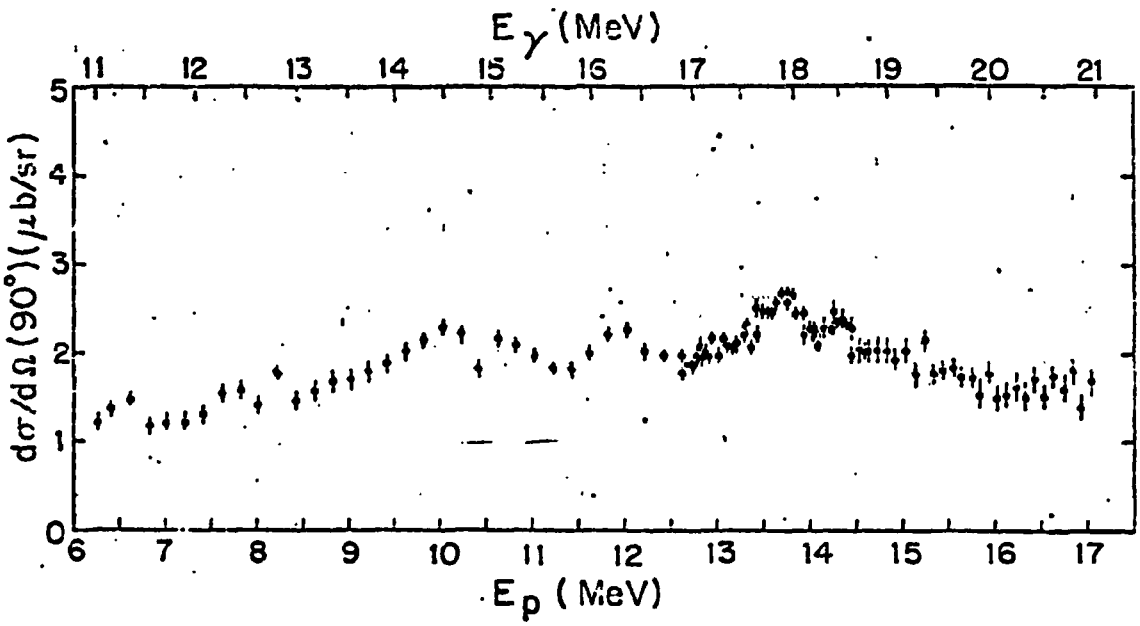

Fig. D2-2 The 90° yield curve for the $^{13}C(p,\gamma_1)^{14}N$ reaction.

tion exhausts approximately 6 percent of the classical dipole sum rule in the region of 13.3 to 23.3 MeV excitation. The transition to the first excited state exhausts about 9 percent of the classical dipole sum rule between 11.0 and 21.0 MeV excitation.

Angular distributions of both the cross section and the analyzing power were also obtained for these two reactions at twelve energies which span the giant dipole energy region. The cross section was measured at nine angles between 30° and 154°, while the analyzing power was measured at seven angles between 42° and 142°. These data were expanded in Legendre and Associated Legendre Polynomials as follows:

$$\sigma(\theta) = A_0 \left[1 + \sum_k A_k Q_k P_k (\cos\theta)\right]$$

and

$$\frac{A(\theta)\sigma(\theta)}{A_0} = \sum_{k=1}^{4} b_k Q_k P_k' (\cos\theta) \quad .$$

The resulting a_k and b_k coefficients are shown in Fig. D2-3 and Fig. D2-4.

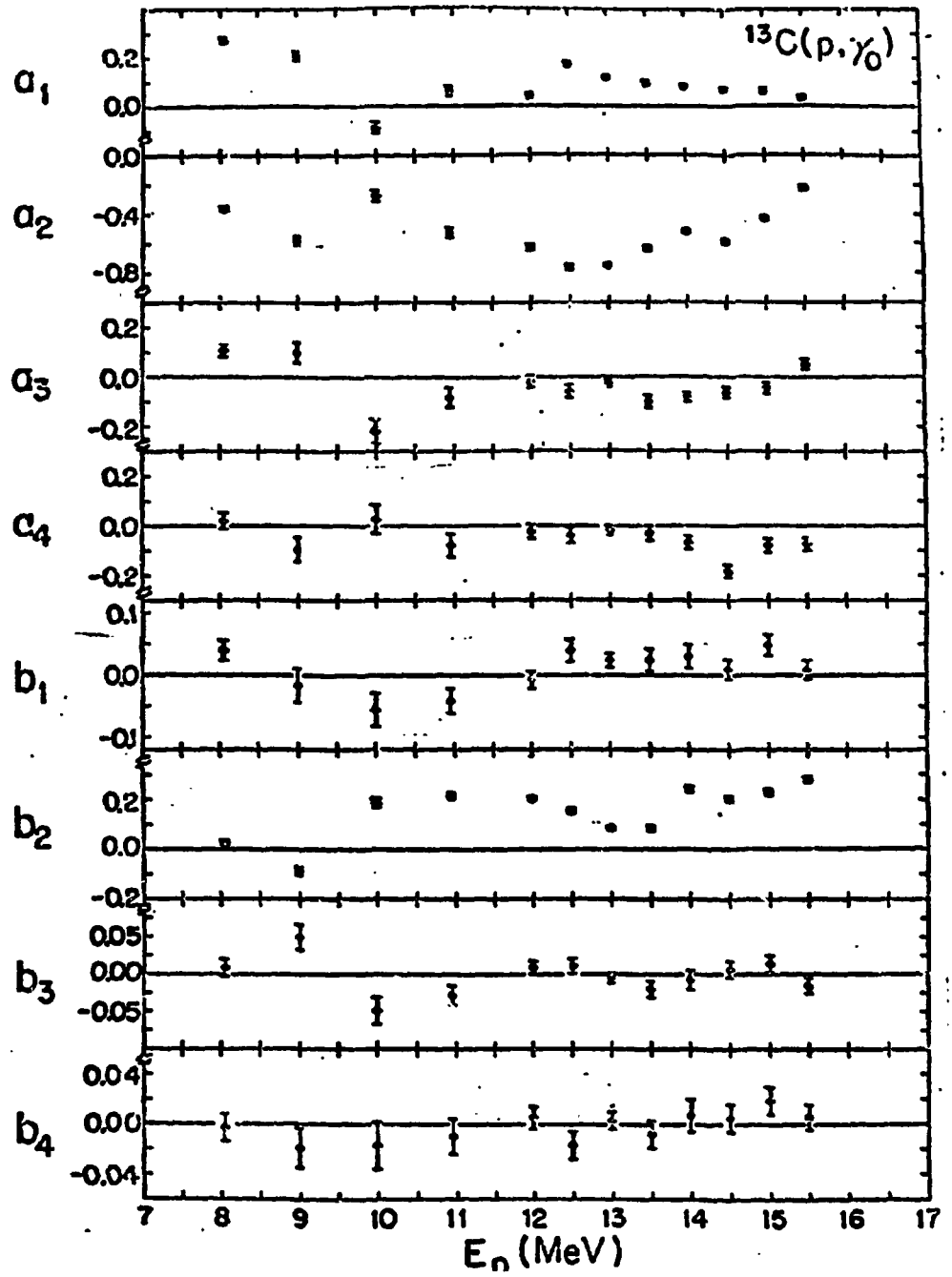

Fig. D2-3 Plots of the a_k and b_k coefficients obtained from fits to $^{13}C(p,\gamma_0)^{14}$ angular distribution data.

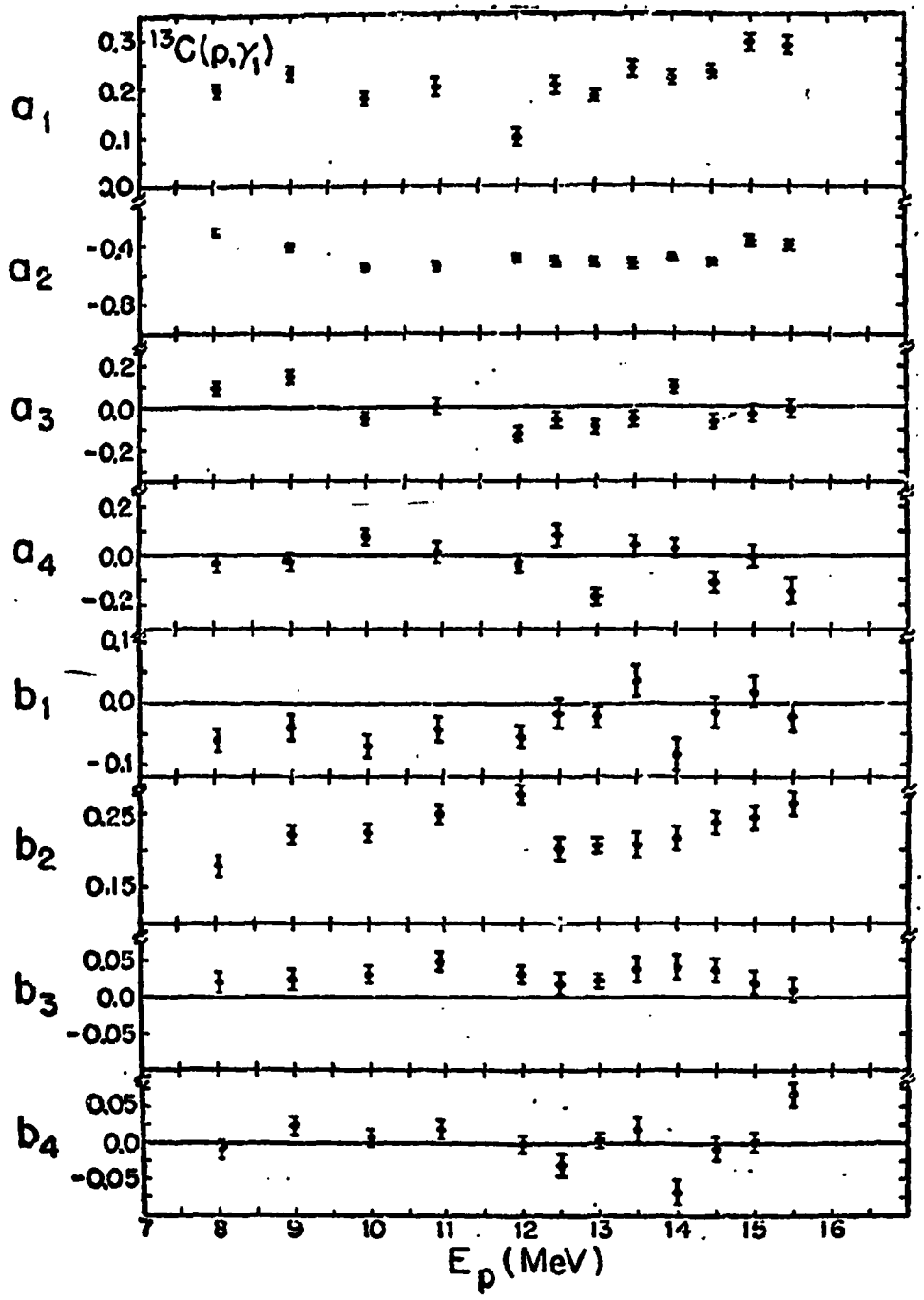

Fig. D2-4 Plots of the a_k and b_k coefficients obtained from fits to $^{13}C(p,\gamma_1)^{14}N$ angular distribution data.

Since the $^{13}C(p,\gamma_1)^{14}N$ reaction leads to a final state with spin zero, the analysis is more straightforward than for the $^{13}C(p,\gamma_0)^{14}N$ case. In the case of (p,γ_1), if we consider only E1 radiation we can express the relevant a_k and b_k coefficients in terms of the T-matrix amplitudes and phases as follows:

$$1.0 = 0.75(s_{1/2})^2 + 0.75(d_{3/2})^2$$

$$a_2 = 1.061(s_{1/2})\,(d_{3/2})\cos(\phi_s - \phi_d) - 0.375(d_{3/2})^2$$

$$b_2 = 0.5303(s_{1/2})\,(d_{3/2})\sin(\phi_s - \phi_d)$$

These equations were solved to determine the $s_{1/2}$ and $d_{3/2}$ amplitude and the relative phase from the experimental values of a_2 and b_2. The results are shown in Fig. D2-5. There are clearly two solutions, one of which is primarily $d_{3/2}$ strength

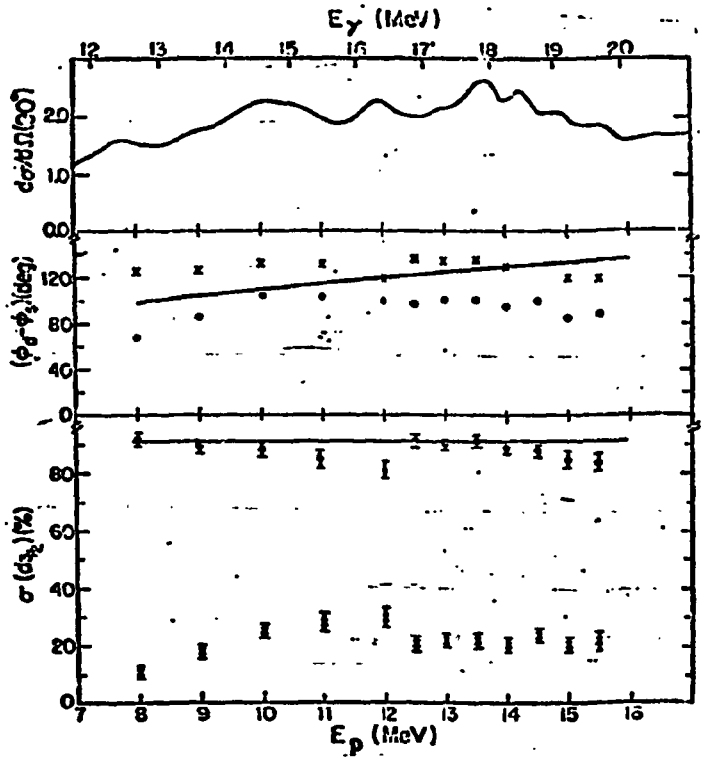

Fig. D2-5 Solutions obtained from a pure E1 analysis of the $^{13}C(p,\gamma_1)^{14}N$ data.

the other primarily $s_{1/2}$ strength.

A calculation using the simplified direct-semidirect model (form factor$\propto$r),[1] was performed for this case. The results are shown in Fig.D2-5. The calculation clearly favors the primarily $d_{3/2}$ solution and accounts for the relative amplitude and phase behavior rather well.

[1] Phys. Rev. C18 (1978) 65

Since the coefficients a_1, a_3, a_4, b_1, b_3, b_4 are non-zero, it is clear that radiation other than E1 is present. The most reasonable next step is to allow for the possibility of E2 radiation. This introduces--in this case of $^{13}C(p,\gamma_1)^{14}N$--two additional T-matrix elements: $p_{3/2}$ (E2) and $f_{5/2}$ (E2) with phases ϕ_p and ϕ_f, respectively. Equations for A_0, $a_1 - a_4$ and $b_1 - b_4$ can now be written down in terms of the four amplitudes (2E1's and 2E2's) and three relative phases. These four amplitudes and three relative phases were fitted directly to the experimental data through the minimization of chi-squared, calculated as follows:

$$\chi^2 = \sum_{data} \left(\frac{1}{\Delta\sigma_i}\right) \left[\sigma_i - \sum_k a_{k\,calc}\, Q_k\, P_k(\cos\theta)\right]^2$$

$$+ \sum_{data} \left(\frac{1}{\Delta\sigma_i A_i}\right) \left[\sigma_i A(\theta_i) - \sum_k b_{k\,calc}\, Q_k\, P_k'(\cos\theta)\right]^2$$

$$\text{where } \sigma_{exp}(\theta_i)/A_0 = \sigma_i$$

The quantities a_{calc} and b_{calc} are calculated from the equations for a_k and b_k written in terms of the complex T-matrix elements. The minimum of χ^2 is obtained with a gradient search routine, and the errors are derived from the error matrix.

Solutions were found at each energy with E1 amplitudes similar to the two pure E1 solutions previously described. Since the DSD calculation indicated that the physical solution was predominantly $d_{3/2}$ capture, the remaining discussion will consider only those solutions.

A search was conducted to determine if multiple solutions exist for the two E2 amplitudes. To do this, the $f_{5/2}$(E2) amplitude was held fixed and the remaining six parameters were varied for a minimum of χ^2. The cross section resulting from the $f_{5/2}$ amplitude was then varied from 0 to 20 percent of the total cross section in 1 percent steps. This was done at all measured energies. Fig. D2-6 shows a plot of

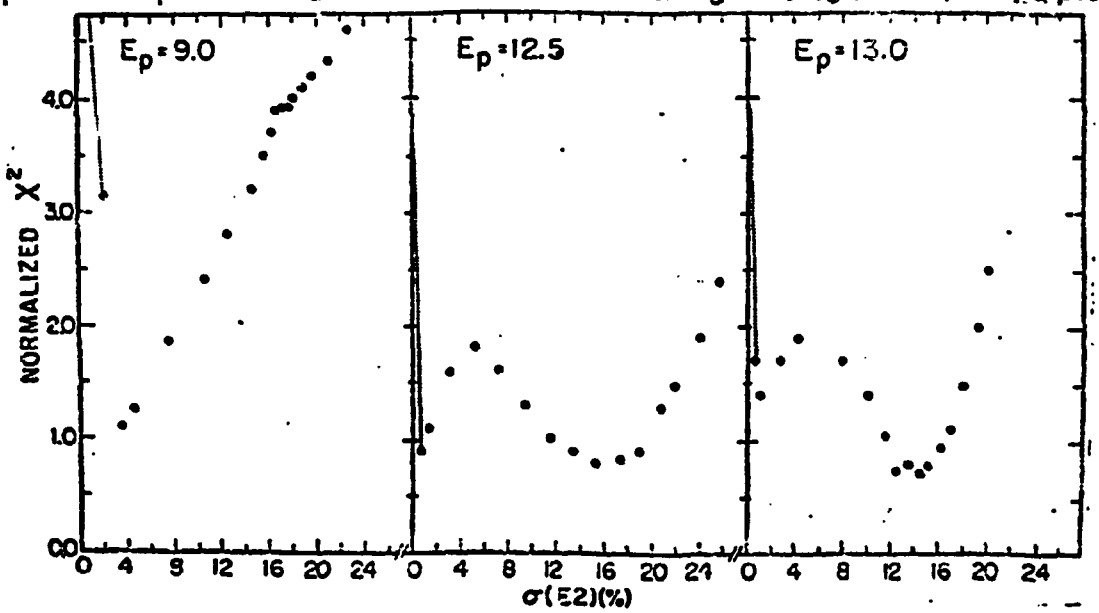

Fig. D2-6 Plots of Chi-Squared as a function of the E2 cross section obtained from an E1-E2 analysis of $^{13}C(p,\gamma_1)^{14}N$ data.

chi-squared per degree of freedom as a function of total E2 strength for three representative energies. The E2 strength is plotted as a percent of the total cross section.

Figure D2-7 shows a plot of the f amplitude and the f- to p-phase differ-

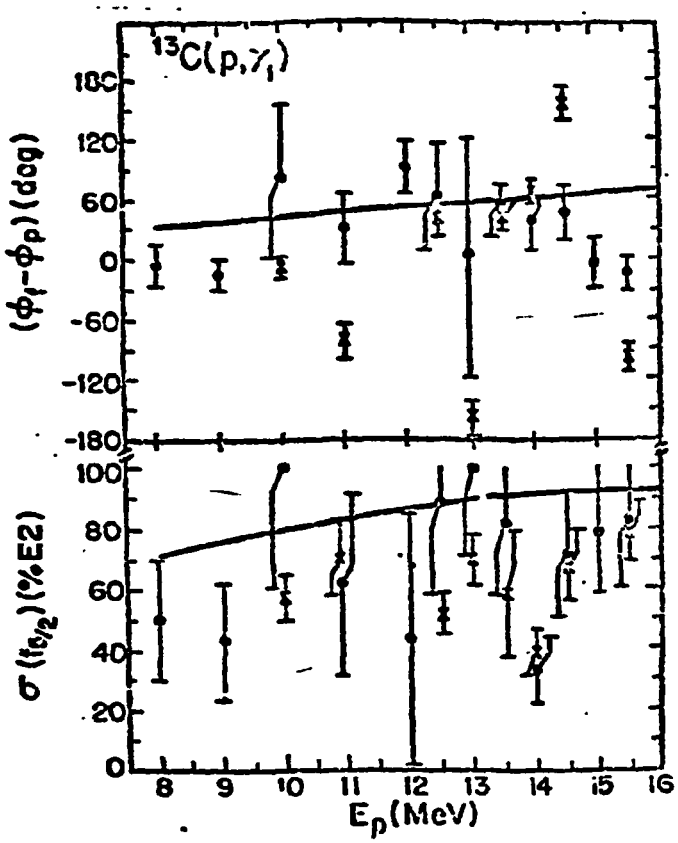

Fig. D2-7 Plots of the E2 amplitudes and relative phase extracted from $^{13}C(p,\gamma_1)^{14}N$ data.

ence as a function of energy. The f amplitude is plotted as a percent of the E2 cross section. The smaller E2 solutions are plotted as points while the larger ones are plotted as crosses. The results of the DSD calculation are shown as solid lines. There appears to be reasonably good agreement between the calculation and the smaller E2 solution.

The total E2 cross section found in our analysis is presented in Fig. D2-8. The solid line is the result of a calculation which assumes that only direct E2 radiation is present. It is apparent that the set of solutions with the smaller E2 cross section is in fair agreement with the pure direct E2 calculation. Although the experiment cannot rule out the larger E2 solutions, we find that they imply an exhaustion of over 100% of the E2 (ISEW) sum rule. We therefore conclude that the smaller E2 solution is preferred, and that if the isoscalar GQR has any strength in the ground state proton channel, its effects are too small to be observed in the present experiment above the E2 background which results from direct (non-collective) capture.

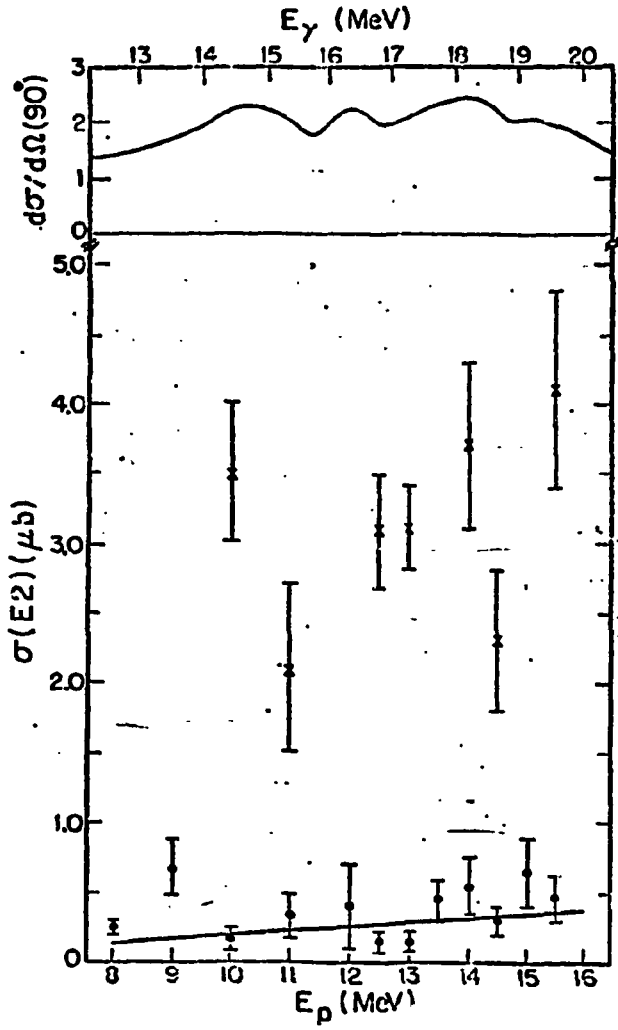

Fig. D2-8 The E2 cross section extracted from $^{13}C(p,\gamma_1)^{14}N$ data.

3. Measurements of The Reactions $^{15}N(\gamma,d_0)^{13}C$ And $^{13}C(\vec{d},\gamma_0)^{15}N$ in The Giant Resonance Region (D.M. Skopik, J.J. Murphy, II, H.R. Weller, R.A. Blue, N.R. Roberson, S.A. Wender, D.R. Tilley)

This work is the result of a collaborative effort between TUNL and the Saskatchewan Accelerator Laboratory. It has been prepared for publication. The abstract follows:

> "The reactions $^{15}N(\gamma,d_0)^{13}C$ and $^{13}C(\vec{d},\gamma_0)^{15}N$ have been measured and compared with previous results. A broad resonance was observed at $E_x \cong 21.9$ MeV in the (γ,d_0) channel. Vector polarized deuterons were used to measure the angular distribution of gamma rays at this resonance. The results were analyzed assuming that the two S = 1/2 E1 transition matrix elements are dominant."

The (γ,d_0) measurements, and the present (d,γ_0) measurements, give absolute cross sections which agree within their estimated errors of ±12%. Furthermore, these results indicate that the original (d,γ_0) measurements[1] should be normalized up-

[1] H.R. Weller and R.A. Blue, Nucl. Phys. A211, 221 (1973)

wards by a factor of 2.5, in agreement with the conclusion of Ref. 2. (Note: the shape of the yield curve of Ref. 1 has been reproduced in Ref. 3.)

The polarized deuteron capture data were analyzed by assuming pure E1 radiation and by assuming that the dominant transition matrix elements would be those having $S = 1/2$: $(LS; J) = (1\ 1/2;\ 1/2)$ and $(1\ 1/2;\ 3/2)$. If the ground state of ^{15}N is pictured as $^{13}C + d$ with an $L = 0$ deuteron, this assumption should be reasonable. The results of our analysis produce two solutions at $E_x = 21.9$ MeV. They are presented in Table D2-1.

Table D2-1

	% Contribution		Relative Phase
Solution I	(J = 1/2)	6 ± 3	$\phi_{3/2} - \phi_{1/2} = 43° \pm 14°$
	(J = 3/2)	94 ± 4	
Solution II	(J = 1/2)	73 ± 7	$\phi_{3/2} - \phi_{1/2} = 22° \pm 6°$
	(J = 3/2)	27 ± 6	

4. Study of The Giant Dipole Resonance Region of ^{60}Ni (J.D. Turner,* C.P. Cameron,** N.R. Roberson, H.R. Weller, D.R. Tilley)

This work has been completed. It was published in Physical Review C 17 (1978) 1853, under the title "Polarized Proton Capture on ^{59}Co". The abstract follows:

> "The angular distributions of cross section and of analyzing power for the $^{59}Co(\vec{p},\gamma_0)^{60}Ni$ reaction have been measured throughout the giant dipole resonance region of ^{60}Ni. In addition, the 90° yield curve has been measured for E_p from 5.8 to 16.5 MeV. The data are analyzed to deduce the amplitudes and phases of the T matrix elements involved. Comparison of the results is made to both the dynamic collective model calculation of Ligensa and Greiner and to a direct-semidirect model calculation. The direct-semidirect calculation indicates that the reaction proceeds predominantly via the radiative capture of $d_{5/2}$ protons. Isospin splitting is also discussed."

---

* Now at Eastern Kentucky University, Richmond, Kentucky
** Now at Sandia Laboratories, Albuquerque, New Mexico

[2] W. Del Bianco, S. Kundu and J. Kim, Nucl. Phys. A270, 45 (1976)
[3] W. Del Bianco et al., Can. J. Phys. 56, 3 (1978)

5. Polarized Proton Capture in The Giant Dipole Resonance Region
(H.R. Weller, N.R. Roberson, S.R. Cotanch)

A paper has been published on this work; the abstract follows.

"Measurements of cross sections and analyzing powers are examined for polarized proton capture on ^{14}C, ^{30}Si, ^{54}Fe, ^{56}Fe, ^{58}Fe, ^{59}Co, and ^{88}Sr at energies which cover the giant dipole resonance region. These data are used to extract the relative amplitudes and phases of the contributing E1 T-matrix elements. A typical result exhibits two solutions. Calculations using the direct (or a direct-semidirect) capture model appear to provide a means for choosing the physical solution."

This paper describes the results of an analysis, which assumes pure E1 radiation, of the angular distributions of cross section and analyzing power obtained from polarized proton capture on the seven targets listed in the above abstract. For example, in the case of $^{14}C(p,\gamma_0)^{14}N$, the only angular distribution coefficient present are:

$$a_0 = 1.0 = (s_{1/2})^2 + 2.0\,(d_{3/2})^2 \ ,$$

$$a_2 = -(d_{3/2})^2 - 2.0\,(s_{1/2})\,(d_{3/2})\cos(\phi_s - \phi_d) \ ,$$

$$b_2 = (s_{1/2})\,(d_{3/2})\sin(\phi_s - \phi_d) \ ,$$

were $s_{1/2}(d_{3/2})$ represent the amplitude of the transition matrix elements for capture of an incoming $s_{1/2}(d_{3/2})$ proton, and $(\phi_s - \phi_d)$ is the relative phase between the two amplitudes. As a result of the quadratic nature of the above equations, the analysis always yields two solutions. For the case of $^{14}C + p$, we find one solution which indicates that approximately 90%(10%) of the cross section is due to $d_{3/2}(s_{1/2})$ capture and a second solution with approximately 20%(80%). Similar results were obtained for all cases, if spin-flip terms, when present, are ignored.

In the direct-semidirect (DSD) reaction model, the evaluation of the transition matrix elements requires the calculation of a radial matrix element having the form

$$\langle \phi_{n\ell j} | r + \frac{V(r)}{E_\gamma - E_d + i\Gamma_d/2} | \chi_{\ell' j'} \rangle$$

where $\chi_{\ell' j'}$ is the proton continuum wave function and $\phi_{n\ell j}$ is the wave function of the valence proton bound in the final state. Since we were interested in obtaining a reliable but simple method for extracting the correct relative amplitudes, we chose to utilize the pure direct model ($V_1(r) = 0$) for the E1 capture calculations.

There are two main conclusions from this work. First: these simple calculations do predict a result which is close to one of the possible solutions for a number of target nuclei. Even though there are discrepancies between the calculated

and experimentally determined phase differences at lower energies, it does appear that one can safely choose the physical solution on the basis of these calculations. Second: the surprising success of the pure direct model in predicting (to first order) the measured angular distributions (equivalently the relative amplitudes and phase of the T-matrix elements) indicate that we are observing the effects of the energy dependence of the proton continuum wave functions. So, although the GDR is essential in order to account for the magnitude of the cross sections, its presence does not show up very dramatically in the proton capture angular distributions.

6. Inelastic Alpha Cross Sections in The Region of The GQR for Nuclei Near Mass 60 (H.R. Weller, S. Manglos, S. Wender, N.R. Roberson, D.R. Tilley, M. Potokar)

A manuscript has been prepared for publication. The abstract follows:

> "Cross sections have been measured for the (α,α') reaction leading to the first excited (2^+) state for targets of ^{52}Cr, ^{54}Fe, ^{58}Fe and ^{60}Ni. Data were obtained at several angles as a function of E_α in the region of 8 to 18 MeV. These energies cover the isoscalar GQR of the composite nuclei--^{56}Fe, ^{58}Ni, ^{60}Ni and ^{64}Zn. It has recently been reported that this GQR of ^{58}Ni, ^{60}Ni and ^{62}Ni decays primarily by alpha emission. While the present data can be interpreted as being consistent with this result, alternative explanations cannot be ruled out."

A typical data set is shown in Fig. D6-1. These data show a peak which has a position, width and strength consistent with a GQR which decays primarily by α emission to the 2^+ state. Other interpretations are possible and are discussed in the manuscript.

7. Study of GDR of ^{89}Y via The Reaction $^{88}Sr(p,\gamma)^{89}Y$ (R.D. Ledford, C.P. Cameron, N.R. Roberson, D.G. Rickel, H.R. Weller, R.A. Blue, D.R. Tilley)

This work was described in Section F-8 of the previous report (TUNL XVI). It is being prepared for publication and should be ready for submission early in 1979.

8. A Search for The Isovector E2 Resonances in ^{31}P, ^{89}Y and ^{60}Ni (N.R. Roberson, H.R. Weller, R.A. Blue, C.P. Cameron, R.D. Ledford, J.D. Turner, S.A. Wender, S. Manglos, D.R. Tilley)

The injector cyclotron is scheduled to be in operation again in January 1979 following the long period necessary for replacement of the main coils.

We plan to resume work on the search for isovector E2 resonances at that time.

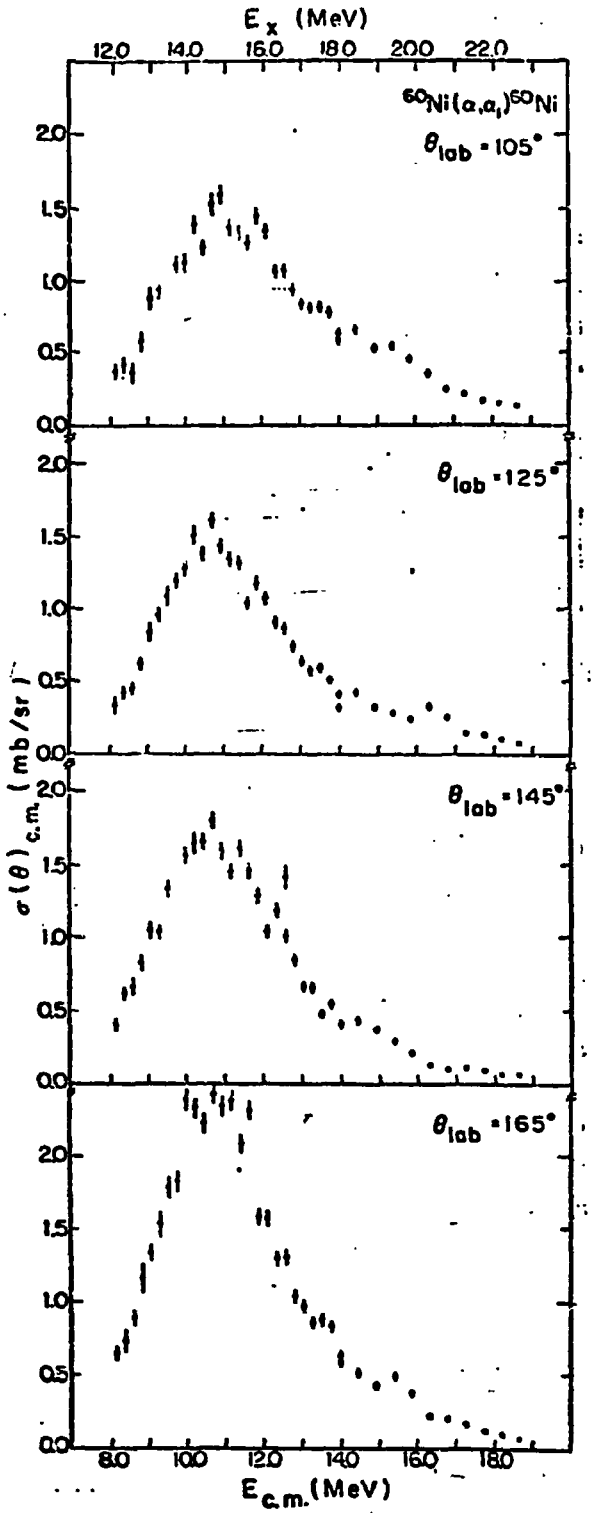

Fig. D6-1 Inelastic alpha cross section for ^{60}Ni in the region of the GQR.

9. Study of The Giant Dipole Resonance Region of ^{31}P (C.P. Cameron, R.D. Ledford, N.R. Roberson, D.G. Rickel,* H.R. Weller, D.R. Tilley)

The results of this study were described in Section F-4 of the previous report (TUNL XVI). A manuscript is being prepared for publication.

10. A Study of The GDR in ^{15}N Using Fast Neutron Capture (S.A. Wender, M. Jensen, M. Potokar, N.R. Roberson, D.R. Tilley, H.R. Weller)

As pointed out by Abert, George and Überall,[1] no measurements have been reported for the $^{15}N(\gamma,n)^{14}N$ reaction. Such measurements may provide additional tests of shell model studies of the giant dipole resonance of ^{15}N. Furthermore, since the ground state of ^{14}N has $T = 0$, the $^{14}N(n,\gamma)^{15}N$ reaction should only populate $T = 1/2$ states of ^{15}N (whereas $^{14}C(p,\gamma)^{15}N$ can, in principle, populate both $T = 1/2$ and $T = 3/2$ states). Hence a study of the $^{14}N(n,\gamma)^{15}N$ reaction could help in sorting out the isospin makeup of the GDR of ^{15}N.

In order to obtain greater accuracy and to extend the measurements to lower energies, we have remeasured the excitation function of the $^{14}N(n,\gamma_0)^{15}N$ reaction over the GDR of ^{15}N. The results of these measurements are shown in Fig. D10-1, along with the previously reported measurements on $^{14}C(p,\gamma_0)^2$ and $^{14}N(p,\gamma_0)$.[3] The errors shown for the $^{14}N(n,\gamma_0)$ reaction on the plot do not include an overall 20% error in the absolute cross section. All data have been detailed, balanced and plotted as a function of excitation energy. It is clear from this figure that the $^{15}N(\gamma,p_0)^{14}C$ cross section ($T = 1/2$ and $T = 3/2$) is larger in magnitude and exhibits more structure than either the $^{15}N(\gamma,n)^{14}N$ or the $^{15}O(\gamma,p)^{14}N$ reactions. We also observe that the $^{15}O(\gamma,p)^{14}N$ and the $^{15}N(\gamma,n)^{14}N$ cross sections are very similar in magnitude and shape. In fact, if the $^{15}N(\gamma,n)$ data are shifted down by about 500 keV the positions of the minima and maxima line up quite well with the $^{15}O(\gamma,p)$ data. It is interesting to note here that if the energy difference between corresponding $T = 1/2$ levels in ^{15}N and ^{15}O is plotted as a function of excitation energy, a linear extrapolation suggests an energy difference of about 500 keV in the vicinity of $E_x = 18$ MeV. These observations support the notion that the $^{15}N(\gamma,n)$ and $^{15}O(\gamma,p_0)$ reactions are exhibiting the $T = 1/2$ strength of the GDR in the mirror nuclei ^{15}N and ^{15}O, while the $^{15}N(\gamma,p_0)^{14}C$ reaction displays both $T = 1/2$ and $T = 3/2$ strength.

In addition to these data we have obtained angular distributions at eight neutron energies between 6 and 13 MeV. These data, obtained at 7 angles, were fitted to an expansion in terms of Legendre polynomials. We are presently in the process of correcting the fits for the effects of finite target size. Satisfactory fits were obtained with the fits through order two. The resulting a_1 coefficients were quite small (typically $-.02 \pm .06$). This is in sharp contrast to the a_1 coefficients reported at corresponding excitation energies in the $^{15}O(\gamma,p_0)$ reaction (where a_1 ranged from .22 to .50 for E_x in the range of 14 to 24 MeV). This observation could be understood if the a_1 coefficient seen in the $^{15}O(\gamma,p)^{14}N$ reaction arose from interference between the dominant E1 radiation and a direct E2 contribution. If this occured one would expect a much smaller a_1 in the $^{15}N(\gamma,n_0)$ data due to the

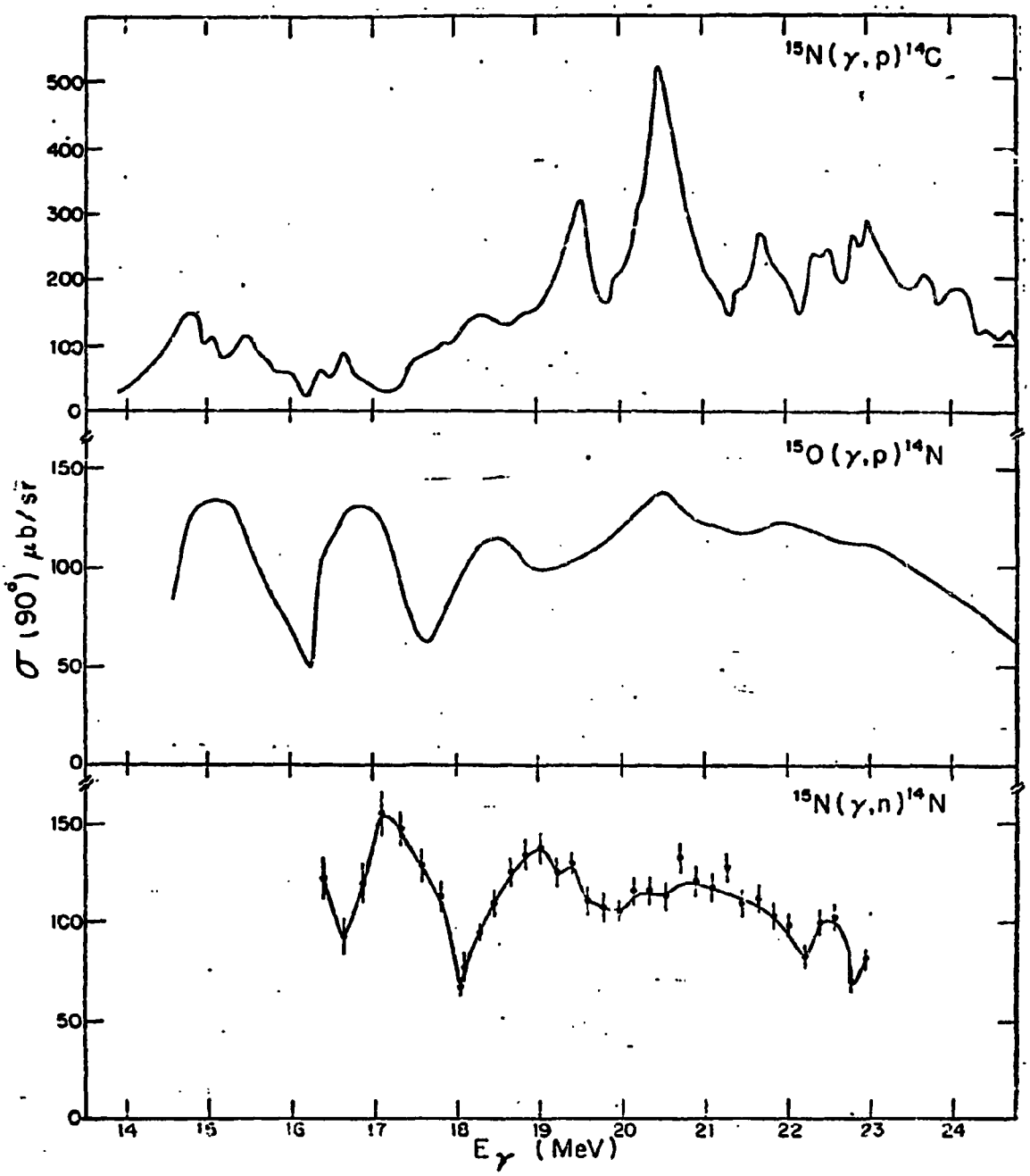

Fig. D10-1 Excitation function for $^{15}N(\gamma,p)^{14}C$, $^{15}O(\gamma,p)^{14}N$ and $^{15}N(\gamma,n)^{14}N$ obtained by detailed balance from the respective capture-reaction data.

fact that the direct E2 strength would be reduced by a factor of the order of Z/A^2, arising from the small quadrupole effective charge of the neutron. Calculations based on the DSD model are underway to further investigate this thesis.

The a_2 coefficients obtained from these data are shown in Fig. D10-2

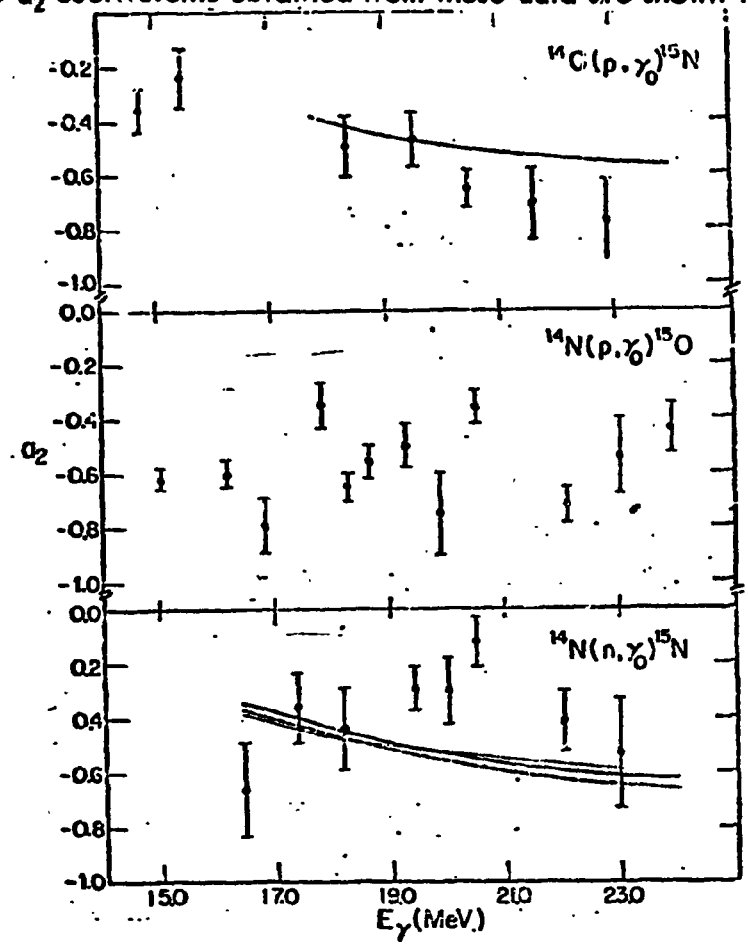

Fig. D10-2 Plots of a_2 coefficients obtained from $^{14}C(p,\gamma_0)^{15}N$, $^{14}N)p,\gamma_0)^{15}O$, and $^{14}N(n,\gamma_0)^{15}N$ data.

along with those obtained from the previously measured $^{14}N(p,\gamma_0)^{15}O$ reaction. Due to the spin-one target both the $^{14}N(p,\gamma_0)$ and the $^{14}N(n,\gamma_0)$ reactions have five E1 transition matrix elements. In a j-j coupling representation two of these correspond to projectiles having $s_{1/2}$ partial waves, two to $d_{3/2}$ partial waves and one to $d_{5/2}$. In a spherical DSD model the $d_{5/2}$ contribution will not contribute. The results of a direct calculation assuming a single $s_{1/2}$ and a single $d_{3/2}$ transition matrix element are shown as the solid lines in Fig. D10-2. Although the magnitude and general trend of a_2 is represented by this calculation, the data suggest an energy dependence in the region around 20 MeV which is not contained in this first order calculation.

Also shown in Fig. D10-2 are the results of a preliminary semi direct calculation using both a real and a complex form factor similar to those described in section D-6. This calculation includes an E1 resonance at 22.5 MeV with $\Gamma = 5.5$ MeV. The fraction of the E1 sum rule is taken from Bezic et al.[1] As shown in Fig. D10-2 this calculation also reproduces the general trend of the a_2 coefficients.

11. Quadrupole Radiation in ^{40}Ca Fast Neutron Capture (S.A. Wender, N.R. Roberson, M. Potokar, H.R. Weller, D.R. Tilley)

A paper on this work has been published (Physical Review Letters 41 (1978) 1217) and a talk presented during the Third International Symposium on Neutron Capture Gamma-rays Spectroscopy which was held at Brookhaven National Laboratory, September 1978. The following is the abstract of the paper.

> "Differential cross sections have been measured for the reaction $^{40}Ca(n,\gamma_0)^{41}Ca$ at seven angles in 1 MeV steps and at $\theta_{lab} = 90°$ in 200 keV steps for incident neutron energies of 6-13 MeV. The extracted a_2 coefficients and the fore-aft asymmetry are in good agreement with a direct-semidirect model calculation if the isoscalar giant quadrupole resonance is included."

The fast neutron capture facility used for this work was described in detail in a previous report (Annual Report - TUNL XVI, Section F-12). Briefly, the neutron source utilized the $^2H(d,n)^3He$ reaction with a pulsed beam incident upon a gas cell. The Ca target was a cylindrical, 3.8 x 3.8 cm ingot. The γ-ray spectrometer consists of our 25.4 x 25.4 cm NaI scintillator with an anticoincidence shield. Only events with proper time-of-flight were stored by the on-line computer, and this provided an effective discrimination against neutron induced background. The eight angular distributions obtained in this work are shown in Fig. D11-1. Each data point represents ~2.5 hours of running time. In Fig. D11-2, the 90° yield curve, the a_2 coefficients, and the fore-aft asymmetry coefficients, a_5, are presented. Assuming E1 and E2 radiation and neglecting a_4, we can write $a_5 = 0.57a_1 - 0.39a_3$.

An extended DSD model[2] which includes quadrupole as well as dipole processes was used to calculate $\sigma(90°)$, a_2 and a_5. The results are shown as solid lines in Fig. D11-2. For the dipole term the coupling interaction of Ref. 3 was used and is proportional to $r\,U_1(r)$ where $U_1(r)$ is the complex optical-model symmetry potential. The quadrupole particle-vibration coupling had a surface-peaked shape proportional to $-r\,d\,U_0/dr$ where $U_0(r)$ is the real central potential. The curves labelled a and b in Fig. F12-2 are for $V_V/W_V/V_0 = 90/45/50$ and $75/37/50$ MeV, respectively. Also

---

[1] N. Bezic, D. Brojnik, D. Jomnek, and G. Kenee, Nucl. Phys. A128 (1969) 426
[2] A. Likar et al., Nucl. Phys. A298 (1978) 217
[3] M. Potokar, Phys. Lett. 46B (1973) 346

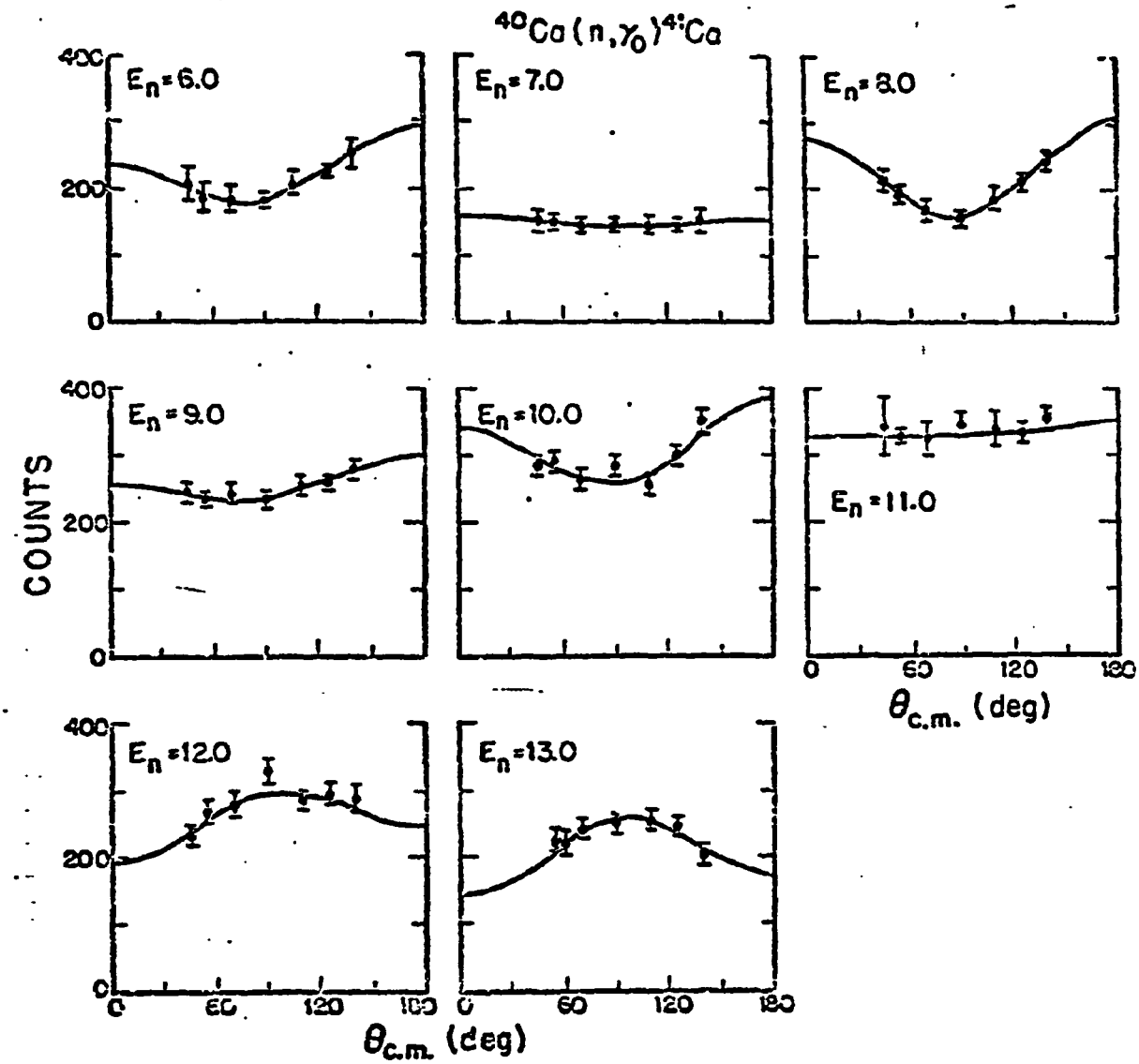

Fig. D11-1 Angular distributions obtained from the $^{40}Ca(n,\gamma_0)^{41}Ca$ reaction.

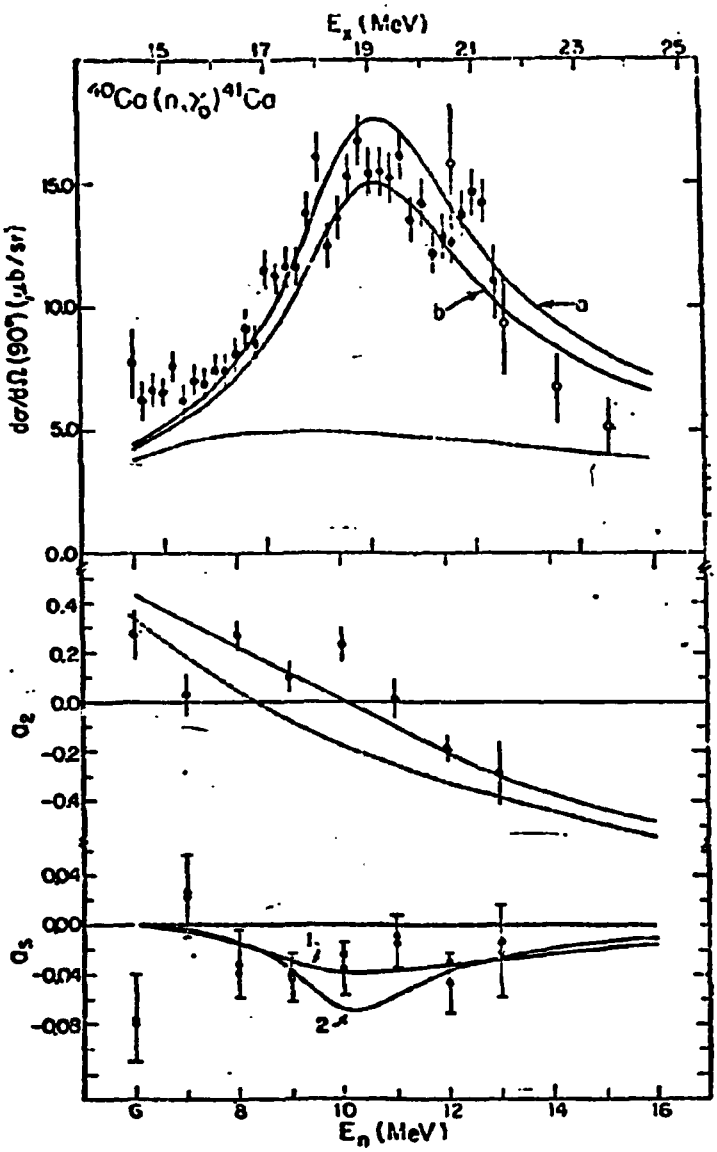

Fig. D11-2 Comparison of the a_2 coefficients, a_s coefficients and 90° yield curve with a DSD reaction-model calculation as described in the text.

$\Gamma_1 = 4.0$ and $E_1 = 18.4$ MeV. The values for E_{20}/Γ_{20} were obtained from inelastic α scattering[1] (curve 1) and from inelastic ^{3}He scattering[2] (curve 2) and are 18.0/4.0 and 18.2/2.2 MeV, respectively. The dashed curves shown for $\sigma(90°)$ and the a_2-coefficients are from a calculation assuming only a pure dipole term.

The results of a calculation of the fore-aft asymmetry, a_s, which include the DSD dipole terms and only a direct quadrupole term are shown as a dashed line in Fig. D11-2. The almost-zero values result from the small neutron quadrupole effective charge of Z/A^2. General agreement with the experimental values of a_s is obtained when the collective quadrupole resonance is included using either set of quadrupole parameters (case 1 and 2). It was, however,

[1] D. H. Youngblood et al., Phys. Rev. C13 (1976) 994
[2] T. Yamagata et al., Phys. Rev. Lett. 40 (1978) 1028

necessary to reduce the value of the collective quadrupole matrix element for case 1 from 43% to 30% of the EWSR. The reported value of 26% was used from case 2.

12. A Study of The $^{40}Ca(\vec{n},\gamma_0)^{41}Ca$ Reaction (M.J. Jensen, S.A. Wender, T.B. Clegg, M. Potokar, N.R. Roberson, D.R. Tilley, H.R. Weller)

To complement and extend our recent measurements of fast neutron capture on ^{40}Ca (Section D-11), we have initiated a program to produce a dc beam of polarized neutrons for use in studying the $^{40}Ca(\vec{n},\gamma)^{41}Ca$ reaction. Our first goal is to determine the b_1 and b_2 (and if possible, b_3) coefficients and search for evidence of the isoscalar E2 resonance in the b_1 (and b_3) coefficients. On the basis of the work reported in D-11 we expect b_1 to show a resonance shape with a peak near $E_n = 10.5$ MeV.

During the past two years we have obtained a detailed understanding of the neutron and gamma-ray induced background in our 25 x 25 cm NaI crystal. With a TOF system, we have determined that there is basically no difference in the spectrum in the region of the γ_0 peak with and without the time criterion. Consequently, for the $^{40}Ca(\vec{n},\gamma_0)$ reaction it is possible to use a dc polarized neutron beam and to correct for the background by fitting to the counts above the γ_0 peak. It should be noted that for $E_n \geq 8$ MeV, the background counts are about 5 - 10% of the γ_0 peak, and that for $E_n < 8$ MeV, they are about 10 - 30% with the larger value occuring at 55°.

The polarized neutron beam is obtained via the $^2H(d,n)^3He$ reaction with a gas cell (3 atm) and a polarized deuteron beam ($p_Z = p_{ZZ} = 0.7$). Recent improvements made to the TUNL Lamb shift polarized beam ion source have yielded increased beam current. We now are able to maintain 150 - 175 nA deuteron beams on target. The vector polarization, $p_{ny}(0°)$ of the neutrons produced by the $^2H + d$ reaction is given by[1]

$$p_{ny}(0°) = \frac{\pm(\frac{3}{2})K_y^{y'}(0°)\,p_Z}{1-(1/4)A_{zz}(0°)\,p_{ZZ}} \quad , \qquad (1)$$

where the ± sign applies for spin up/down and p_Z and p_{ZZ} are the vector and tensor polarization relative to the axis of symmetry of the polarized beam ion source. The zero-degree analyzing powers, $A_{zz}(0°)$, and polarization transfer coefficient, $K_y^{y'}(0°)$, have been measured by P. W. Lisowski[1] and have a rather slowly varying energy dependence (typical values are $A_{zz}(0°) = -0.45$ and $K_y^{y'}(0°) = 0.63$ near 8.5 MeV). The neutron vector polarization obtained by this method is from eqn. 1

$$p_{ny} \cong 0.6 \ .$$

Using the same experimental setup as discussed in Section D-11, two runs have been completed. Angular distributions of analyzing power, $A(\theta)$, were measured at 7.5, 8.0, 9.0, 10.0 and 11.0 MeV. Figure D12-1 shows our preliminary

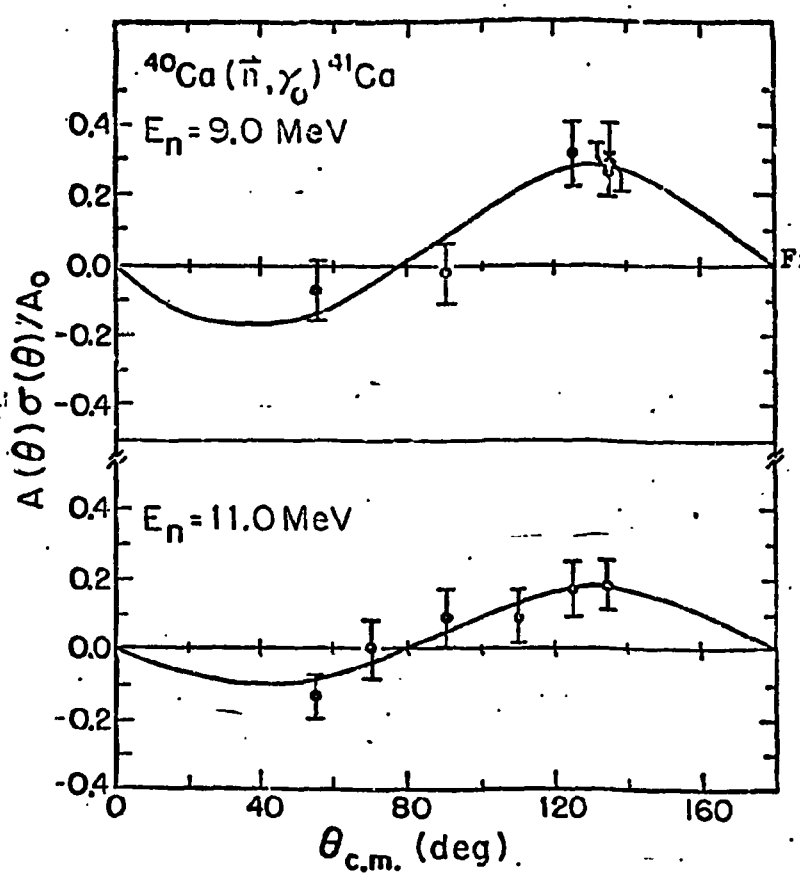

Fig. D12-1 Preliminary data from angular distribution of analyzing power measurements of polarized neutron capture by ^{40}Ca.

results at $E_n = 9.0$ and $E_n = 11.0$ MeV. It is emphasized that these are preliminary results, i.e., no corrections have been made for (1) asymmetries in the forward angle neutron yield due to the deuteron polarization, (2) target multiple scattering which includes polarization effects, and (3) other finite geometry effects.

An experimental estimate of the size of these correction factors was made by measuring $A(\theta)$ at 135° and at $E_n = 9$ MeV using a target 1/6 the volume of our standard target. The result of this measurement is shown as an (x) in Fig. D12-1. Clearly, this result indicates that the final corrections will be a reasonably small fraction of the analyzing powers shown here.

Preliminary values of b_2 are shown in Fig. D12-2 along with the results of a DSD calculation which uses the same parameter as the calculation discussed in Section D-11. A study of the $^{40}Ca(\vec{n},\gamma_0)$ reaction is clearly feasible and more experimental work is planned for the coming year. Besides providing a critical test of the DSD model calculations these measurements may provide confirmation of the isoscalar GQR in ^{41}Ca.

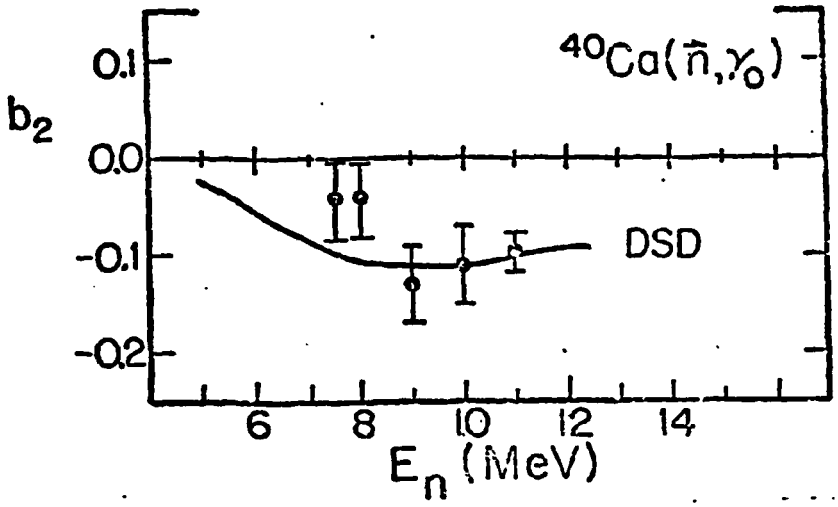

Fig. D12-2 Plots of the analyzing-power distribution coefficient b_2 from analysis of preliminary $^{40}Ca(\vec{n},\gamma_0)^{41}Ca$ data.

13. On The Study of The $^{208}Pb(n,\gamma)$ Reaction (M. Potokar,* M. Jensen, D.R. Tilley, H.R. Weller, S.A. Wender, N.R. Roberson, S. Raman**)

The problem of neutron capture on ^{208}Pb has a long history in the study of the radiative capture process in the GDR region. Yet it seems still to be poorly understood. The observed excitation functions[1] for $^{208}Pb(n,\gamma)$, $^{208}Pb(n,\gamma_1)$, $^{208}Pb(n,\gamma_2+\gamma_3)$ and $^{208}Pb(n,\gamma_5+\gamma_6)$ helped to demonstrate that the physical idea of the DSD model for the nucleon capture dynamics in the GDR region is correct. However, the model calculations have shown also that the shape of the cross section is not reproduced in detail. The experimental excitation functions showed symmetric resonances, while the calculated ones showed higher cross sections on the high energy slope. The complex coupling, introduced to take into account other possible few-step processes in an average way,[3] was found to bring the theory and experiment into better agreement. However, the imaginary part of the coupling was much stronger than that deduced from other reaction data. While the complex nature of the coupling interaction has been justified[3] by deriving the DSD model in the doorway state approximation using Feshbach's unified reaction theory, very little has been done to demonstrate the degree of importance of the imaginary part of the coupling. More experimental data on the detailed shape of the excitation function and on the angular distribution a_2-coefficients are needed, since the nature of the coupling is most strongly reflected in these two quantities.

---

*

**Oak Ridge National Laboratory

1 I. Bergqvist, D.M. Drake, and D.J. McDaniels, Nucl. Phys. A231 (1974) 29
2 M. Potokar, et al., Nucl. Phys. A277 (1977) 29
3 M. Potokar, Phys. Lett 46B (1973) 346, and to be published

We have initiated measurements of the 90° yield curve for the $^{208}Pb(n,\gamma_0)$ reaction in the energy reaction E_n = 7 to 12 MeV in small energy steps. The excitation energies studied cover the high energy side of the GDR. A spectrum is shown in Fig. D13-1. At a few energies a_2 coefficients were obtained for the (n,γ_0) as well as the (n,γ_1) channel. Analysis is underway.

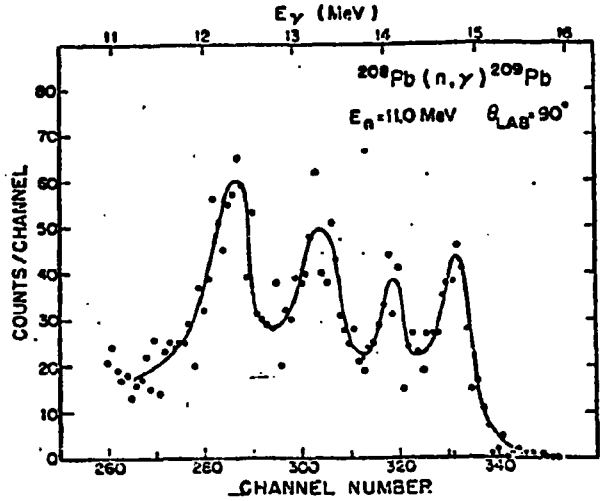

Fig. D13-1 Spectrum from the $^{208}Pb(n,\gamma)^{207}Pb$ reaction.

14. Gamma-ray Spectrometer Calibration (L. Ward, C. Fitzpatrick, M.J. Jensen, S. Manglos, D.R. Tilley, N.R. Roberson, H.R. Weller, S.A. Wender, M. Wright)

A drawing of our gamma-ray spectrometer (and TOF system) is shown in Fig. D14-1. During the past year we have removed 4" of lithium carbonate plus

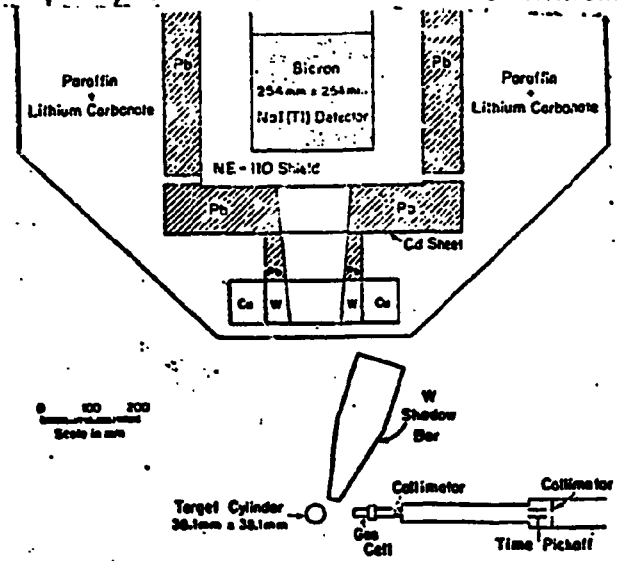

Fig. D14-1 A drawing of the gamma-ray spectrometer as used in neutron capture measurements.

paraffin from the collimator throat. We find that the remaining 8" of Li_2CO_3 plus paraffin gives adequate protection for the NaI crystal from fast neutrons that enter the collimator. For this new arrangement we have remeasured the efficiency (probability ϵ that a photon will be recorded if it reaches the spectrometer) of the detector system.

The thick target (50 keV for 14.2 MeV protons) yield was obtained for the $^{12}C(p,\gamma_0)$ reaction over the 15.07 MeV resonance in ^{13}N. This yield, when combined with the recent measurement[1] which determined that the step in the total thick-target yield corresponds to $(6.83 \pm 0.22) \times 10^{-9}$ γ-rays per incident proton, permits a determination of the product, $\Omega\epsilon$, of the detector solid angle and efficiency. Since it is somewhat more informative to discuss the efficiency alone, we have divided out the solid angle and will present our results in terms of ϵ. It should be kept in mind that the percentage error given for ϵ is in fact the percentage error in $\Omega\epsilon$.

The anticoincidence shield of the spectrometer is viewed by eight XP 1031 phototubes operated at 2000 volts. The anode signal of each tube is amplified by a factor of 4 before mixing. After the mixer circuit there is an additional gain which is variable from 4 to 112. The resulting signal is fed to a fast discriminator the output of which is used to reject all events that occur in both the NaI crystal and anti-coincidence shield. Fig. D14-2 shows the effi-

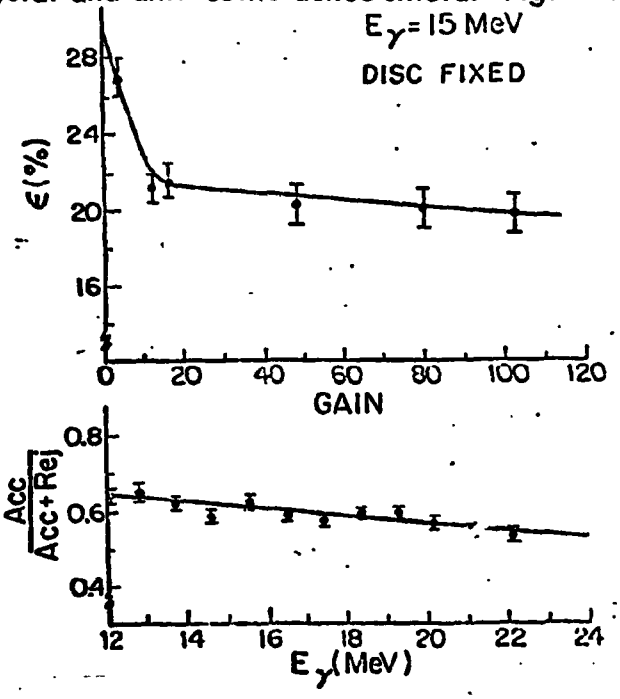

Fig. D14-2 Gamma-ray spectrometer efficiency vs. gain (upper portion) and acceptance ratio vs. gamma energy (lower portion) as discussed in the text.

ciency vs. gain for E_γ = 15.0 MeV when the peak was summed in the full energy region and the discriminator trigger level was kept fixed (EG and G TD101, disc = 023).

The spectrometer efficiencies at other energies have been obtained by correcting for the experimentally determined energy dependence of (1) the crystal response function, (2) the attenuation of the gamma rays by the shielding in front of the crystal, and (3) the rejection rate due to the anti-coincidence shield. The crystal response functions have been obtained from the work of Evans Hayward, W. R. Dodge and B. H. Patrick[1] who have measured γ-ray spectra in a 25 x 25 cm NaI crystal for mono-energetic gamma rays. The attenuation of the gamma rays as a function of energy was calculated using standard cross sections. An accurate measurement of the attenuation for our setup was made at 15 MeV and a small renormalization of the calculated attenuation coefficients was made. The rejection rates were determined for the γ_0 and γ_1 transitions obtained with the $^{13}C(p,\gamma)$ reaction (see Section F-3) and are shown in the lower part of Fig. D14-2. With small extrapolations at the lower and higher energies, we have obtained the spectrometer efficiencies for $10 \leq E_\gamma \leq 25$ MeV.

As a check on our procedures, we have calculated ϵ at E_γ = 15 MeV using item (1), (2) and (3) as discussed above and obtained $\approx$ 19.4% which compares well with the measured value of $\epsilon = (19.8 \pm 1.0)\%$. We have also compared cross sections obtained at TUNL for the $^{13}C(d,\gamma_0)^{15}N$ reaction with those of the $^{15}N(\gamma,d_0)$ reaction measured at the Saskatchewan Accelerator Laboratory.[2] For E_γ = 20 - 25 MeV, we find agreement to about 3% which is well within the stated accuracy of both experiments.

15. Computer Program Development for Neutron Capture Data Correction
(M.J. Jensen, H.H. Hogue, S.A. Wender)

FIXER, a FORTRAN code, has been developed to correct the observed (n,γ) cross sections for finite geometry and neutron multiple scattering effects. These effects include deuteron beam spread and energy loss in the gas cell, $\sigma(\theta)$ for the $^2H(d,n)$ reaction, neutron and gamma ray absorption in the target, and solid angle corrections for both neutron and gamma ray fluxes. The neutron multiple scattering correction procedure takes account of single, double, etc., scatterings of the neutron before an (n,γ) reaction.

---

[1] Evans Hayward, W.R. Dodge, B.H. Patrick, to be published
[2] D.M. Skopik, SAL, private communication

E. ATOMIC PHYSICS

1. Target Thickness Effects in Heavy Ion Collisions (M. Clark, J.M. Feagin, A. Kodre,* J. Swenson, S.M. Shafroth, J. Willis, J.A. Tanis, R. Mowat, A. Waltner)

During 1978 the major progress has been a further study of target thickness effects on both the projectile characteristic and REC x-rays as well as target characteristic x-rays. Using the model of Betz et al. (PRL 33, 807 (1974) to describe the passage of a heavy projectile such as $\overline{Cl^{+F}}$ through a thin film such as Cu, we have obtained sets of parameters for projectile energies of 20, 40, 60 and 80 MeV.

J.A. Tanis gave an invited talk on this work at the small accelerator conference in Denton, Texas, November 6 - 8, 1978. A written version has been accepted for publication in the IEE proceedings of the Fifth Small Accelerator Conference and will appear as a bound volume in 1979.

We plan to submit it for journal publication in the near future. S.M. Shafroth presented it at the International Conference on X-ray and XUV Spectroscopy, Sendai, Japan, August 28 - September 1, 1978. He was invited to give a more detailed presentation at Tohoko University on September 2, 1978. Journal articles (by J.A.T. and S.M.S.) describing two aspects of this work were published this year. The first of these was entitled "Target-Thickness Dependence of Radiative Electron Capture in Heavy-Ion Collisions" and appeared in Phys. Rev. Letters 40, 1174 (1978). The abstract follows:

> "We show how the target-thickness dependence of heavy-ion-induced x-ray production cross sections can be used to normalize the measured K REC (radiative electron capture) intensity to the fraction of incident ions with K vacancies. Experimental REC cross sections for Cl ions on Cu targets are in good agreement with the free-electron theory of Bethe and Salpeter if it is assumed that all of the M- and N-shell electrons in Cu contribute to the REC process."

The second article, entitled "Projectile Fluorescence Yields in Heavy Ion Collisions", was published in Physics Letters 67A, 124 (1978). The abstract follows:

> "Fluorescence yields of highly ionized projectiles entering thin solid foils are determined from a target-thickness analysis of projectile and target K X-ray cross sections. Values are obtained for 20-80 MeV Cl ions on Cu and compared with scaling calculations."

---

* Fulbright fellow from Ljubljana, Yugoslavia

The target thickness dependence of Cl^{10+} and Cl^{16+} K x-ray cross sections along with the calculated curves based on the parameters of the Betz model is shown here in Fig. E1-1.

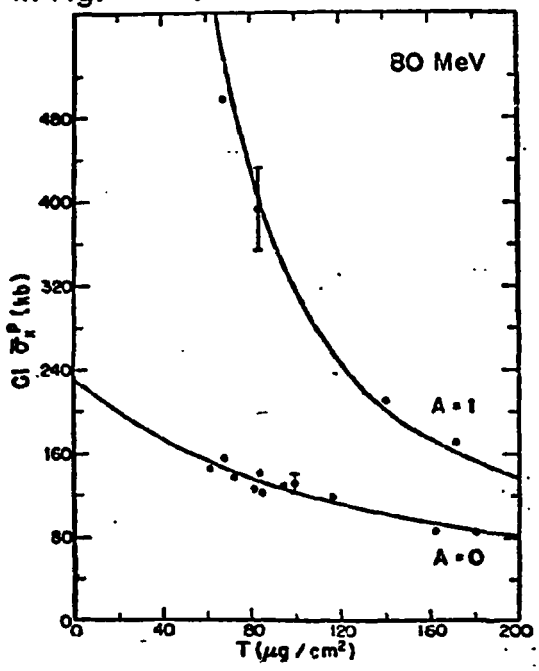

Fig. E1-1 Projectile K x-ray cross section vs. target thickness for 80 MeV Cl^{10+} (A = 0) and Cl^{16+} (A = 1) ions incident on thin Cu coils.

We have also studied Cl^{9+} projectile K_α x-rays under high resolution with a curved crystal vacuum x-ray spectrometer for thin C, Cu and KCl targets and incident energies of 20, 40, 60 and 80 MeV, as well as target Cl K x-rays when projectiles of Cl^{9+}, O^{9+} and protons were incident on KCl. Fig. E1-2 shows typical spectra. A 3-MeV proton beam incident on a KCl target was used

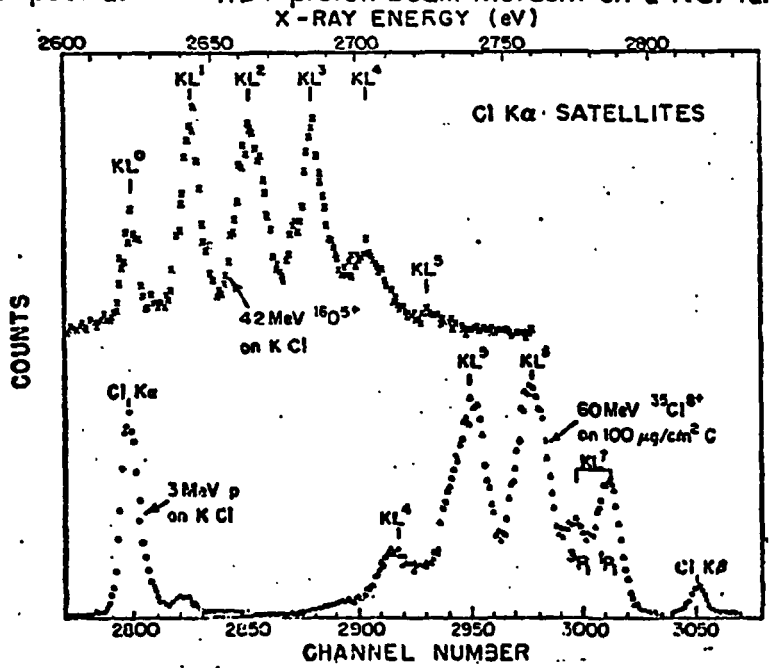

Fig. E1-2 Cl K_α satellites arising from 60 MeV Cl^{8+} ion bombardment of KCl.

to calibrate the spectra. The low energy Cl satellites are clearly seen in the O^{q+} on KCl spectra. These are transitions occurring in the presence of from 1 to 5 L-shell vacancies. The high energy satellites are seen in the spectrum obtained with 60 MeV Cl^{q+} on C. The energies for these peaks must be increased by ~0.2% to compensate for the energy loss due to transverse Doppler effect. A spectrum of Cl K x rays when 60 MeV Cl^{q+} impinges on KCl (Fig. E1-3) shows the full range of satellites - the high energy ones being due to the projectiles, and the low energy ones being due to the target x-rays.

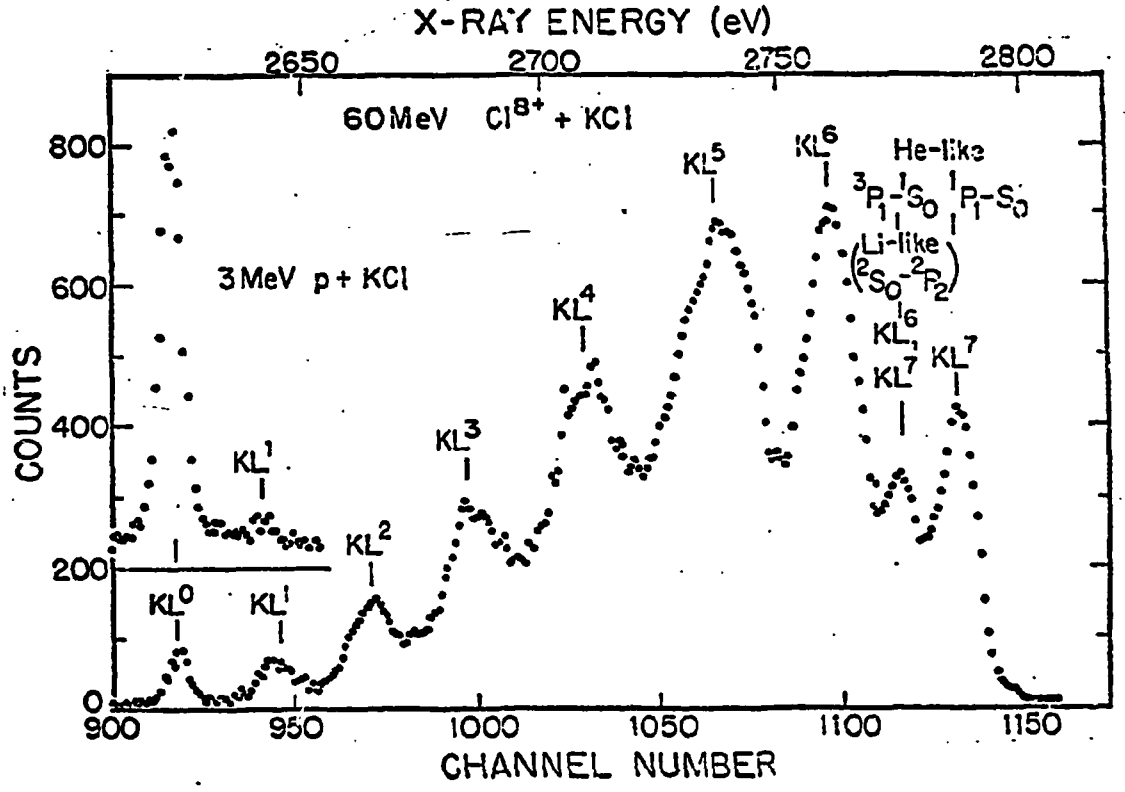

Fig. E1-3 Composite figure showing Cl K_α x-ray satellites. In the upper left is a spectrum of Cl target K_α satellites excited by 42 MeV O^{5+} ion bombardment of KCl. At the lower left and extreme lower right are Cl K_α and K_β spectra resulting from 3 MeV proton bombardment of KCl. The remaining spectrum is Cl K_α satellites from 60 MeV Cl^{8+} ions on Ca target.

The width of the peak labled $KL^7(^1P_1 - {}^1S_0)$ can also be understood in terms of Doppler broadening. A preliminary description of this work was given by S.M.S. at the Southeastern Section meeting of the American Physical Society in Blacksburg, Va., October 28, 1978. The lifetime of the forbidden $^3P_1 - {}^1S_0$ transition can be inferred by studying its intensity as a function of target thickness. So far we have data at 20 and 100 $\mu g/cm^2$.

A further interesting feature of these data is the energy dependence of $P_L(O)$, the probability of simultaneous K and L shell ionization at zero impact parameter.

It may be possible to understand theoretically the experimental values of $P_L(O)$ using non-perturbative calculations of Wu and Merzbacher, and this is being investigated.

2. Resonant Raman X-ray Scattering (A. Kodre, R. Mowat, J. Swenson, S.M. Shafroth)

As part of our effort to study x-ray processes we decided to investigate the recently discovered (1974) Resonant Raman x-ray scattering which can be more important than Compton scattering if the incident x-ray energy is slightly less than the K-shell binding energy of the scatterer.

This work was done with various x-ray tubes, a G. E. spectrogoniometer, a flat LiF crystal (2d = 4.028Å), and Soller slits to obtain monochromatic x-rays with a spread of ~ 30 eV and with variable energy. Scattered x-rays were detected with a Si(Li) detector which has been converted from vertical to horizontal. The results of 120° scattering of near K- edge radiation on a thick Mo target are shown in Fig. E2-1 for incident x-ray energies varying between 2.5 keV and 40 eV below the Mo K

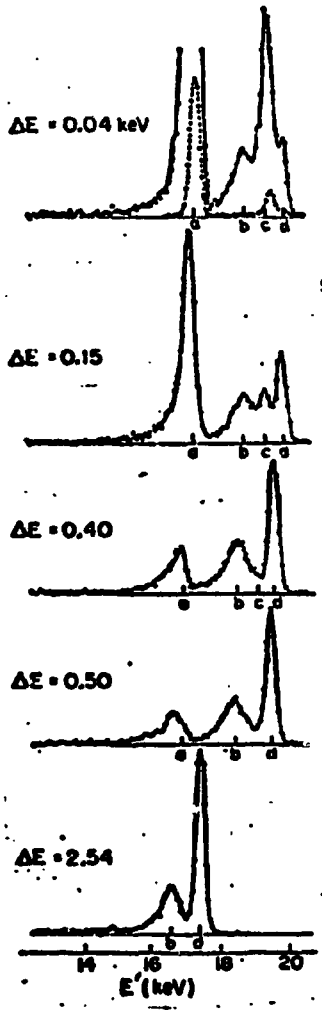

Fig. E2-1 Energy spectra of x-rays scattered at 120° from a thick Mo target in the order (from bottom to top) of increasing energy of the incident radiation shown by the labels $\Delta E = E_K - E$. Arrows a - d on the energy scale point to the calculated positions of the K-L RRS cutoff, the Compton peak, the K-M RRS cutoff, and the elastic peak, respectively. With the uppermost spectrum, a Mo fluorescence spectrum (dashed line - not to scale) is shown to provide a comparison for RRS peak positions. All spectra are normalized to the same incident beam intensity.

edge (19.999 keV). In addition to the previously known K-L Raman scattering where the scattered peak is found at about 17.4 keV (Mo K_α) - ΔE, we found a new peak corresponding to K - M scattering at 19.6 keV (Mo K β_{13}) - ΔE. This was the subject of a paper which has been accepted for publication in Physical Review A. It is entitled "Resonant Raman Scattering of X-rays: Evidence for K-M Scattering". The abstract follows:

> "Resonant Raman x-ray scattering on molybdenum was studied using a Mo-anode x-ray tube and a LiF crystal monochromator. Beside the usual resonant Raman peak corresponding to the fluorescent Kα lines another peak with a smaller energy loss was found. It is attributed to resonant Raman scattering with a final state M-shell vacancy corresponding to the fluorescent Kβ lines. Both contributions are shown to be independent of the scattering angle. Absolute cross sections have been determined and compared with theoretical predictions."

A second paper in which we deduce widths of K - vacancy excited states in a series of elements by comparing the resonant Raman scattering cross section with the above K edge fluorescent spectrum is ready to submit for journal publication. The contents of both of these papers were reported at the International Conference on X-Ray and XUV Spectroscopy at Sendai, Japan and the Small Accelerator Conference at Denton, Texas. The abstract follows:

> "The ratio of the cross section for X-ray fluorescence and the cross section for resonant Raman scattering depends on the width of the intermediate state involved. Thus, a method is developed to determine level widths in a low-resolution experiment. Widths of K-vacancy excited states in Zr, Mo, Rh, Ag, and Sn were determined as (4.0 ± 0.3) eV, (4.6 ± .3) eV, (6.4 ± .5) eV, (7.6 ± .7) eV and (12.0 ± 1.5) eV, respectively, with the apparatus of ~50 eV resolution."

Presently we are searching for shifted Auger electrons following below-edge irradiation of Co with a Ni anode x-ray tube. Photoelectrically ejected Auger electrons are detected with a parallel plate electron spectrometer. The incident x-rays are selectively filtered with a Co absorber so that Ni K_α is the major constituent of the x-ray beam incident on the Co target. Preliminary results appear promising.

A paper by B.L. Doyle and S.M. Shafroth has been submitted to Phys. Rev. A entitled "$L_1 - L_2 M_{4,5}$ and $L_1 - L_3 M_{4,5}$ Coster-Kroning transition thresholds in the Region $37 \leq Z \leq 56$". This paper describes the Ph.D. thesis work of B.L. Doyle. The abstract follows:

"The L_1-L_2 $M_{4,5}$ and L_1-L_3 $M_{4,5}$ Coster-Kronig transition thresholds in the atomic number region $37 \leq Z \leq 56$ are determined by bombardment of these elements with 2.5 MeV H^+ ions and detection of the resulting L X rays with a curved crystal spectrometer. The intensities of both the L_α, $L\beta_1$ and $L\beta_{3,4}$ x rays which are produced during these collisions are dependent on the energetic permissibility of these Coster-Kronig transitions. The discontinuous nature of these intensity ratios as functions of atomic number indicate that the L_1-L_2 $M_{4,5}$ and L_1-L_3 $M_{4,5}$ transitions are energetically allowed for the elements with atomic numbers in the regions $Z \leq 39$ or 40 and $Z \leq 49$ or 50, respectively."

F. HEAVY ION PHYSICS

1. Neutron Emission in Deep Inelastic Scattering Processes

Strongly damped collisions between heavy ions have been studied extensively in recent years. Measurements of neutron emission can determine the excitation energy carried away by each fragment, and determine the time scale of energy equilibration during the collision. Two such measurements have been performed at the UNILAC of GSI, Darmstadt; a feasibility study of the Xe-Au system with a relatively simple experimental setup, and a thorough study of the Kr-Er system with a kinematically complete charged particle identification system and in- and out-of-plane detection of neutrons.

a. Neutron Multiplicities in Inelastic Collisions of ^{132}Xe with ^{197}Au (C.R. Gould,* R. Bass, J. Czarnecki, V. Hartmann, K. Stelzer, R. Zitzmann and Y. Eyal,** ((Institut für Kemphysik, Frankfurt and GSI, Darmstadt)))

A preliminary account of this experiment has been published in Zeit. Phys. A284, 353 (1978). The abstract is given below.

> "The multiplicities of neutrons emitted from the light and heavy fragments, respectively, in the inelastic scattering of 7.5 MeV/amu ^{132}Xe ions from ^{197}Au have been studied as a function of total energy loss. The measured multiplicity ratios are close to the Au-Xe mass ratio for all Q-values, consistent with a rapid thermalization of the excitation energy. The absolute multiplicity values are lower than expected and suggest significant pre-equilibrium effects."

This measurement of multiplicity ratios equal to the Au-Xe mass ratio provided the first direct experimental evidence for a rapid equilibration of the excitation energy in a deep inelastic scattering process. That the absolute multiplicities were ~25% low was less firmly established because of the large experimental errors. We concluded that our results implied non statistical emission of neutrons in the early stages of the collision. The later, more accurate Kr-Er experiment found no evidence for pre-equilibrium effects, however.

To investigate the source of this discrepancy an experimental determination of the neutron attenuation of the chamber and detector material was made at Frankfurt using 5, 10 and 15 MeV neutrons from the $^{2}H(d,n)$ and $^{3}H(d,n)$ reactions. These results indicated that the neutron absorption was underestimated

---

* On leave from N.C. State University, work supported by A. Humboldt foundation, West Germany

** On leave from Weizmann Institute, Rehovot, Israel

by ~10% in our original work, and that the absolute neutron multiplicities should have been ~10% higher.

A more detailed version of the Xe-Au paper is being readied for publication. We believe now that, although the neutron multiplicities are somewhat low, the results are not inconsistent with statistical equilibrium subject to the large experimental uncertainties.

b. Neutron Emission in Strongly Damped Collisions of ^{86}Kr on ^{166}Er at 602 MeV (Y. Eyal, A. Gavron, I. Tserruya, Z. Fraenkel, Y. Eisen, S. Wald ((Weizmann Institute, Rehovot)), R. Bass, C.R. Gould, G. Kreyling, R. Renfordt, K. Stelzer, R. Zitzmann ((IKF, Frankfurt)), A. Gobbi, U. Lynen, H. Stelzer, I. Rode, R. Bock ((GSI, Darmstadt)))

This experiment was performed with a pair of two-dimensional position sensitive parallel plate avalanche counters and an array of eight in- and out-of-plane neutron counters. Using the 250 ps bunched beam facility of the UNILAC at GSI, a mass resolution of ~10 a.m.u. FWHM and an energy resolution of ~50 MeV FWHM were achieved for the outgoing heavy fragments. The results have been described in Phys. Rev. Letters 41, 625 (1978). The abstract appears below.

> "The neutron multiplicity in strongly damped collisions of ^{86}Kr on ^{166}Er was measured at 602 MeV beam energy. The measured ratio of the neutron multiplicities for the light and heavy fragments is in good agreement with the corresponding mass ratio, indicating a sharing of the excitation energy proportional to fragment mass. The results are consistent with predictions of a statistical model calculation assuming evaporation of neutrons from fully accelerated, unpolarized fragments."

Fig. F1-1 shows the neutron multiplicities, ν, as a function of the fragment mass, A, averaged over the c.m. kinetic energy interval $160 \leq E_{cm} \leq 260$ MeV. The quantity ν (A) is the total number of neutrons emitted from both fragments. The solid lines are the results of evaporation calculations. The upper right hand corner shows the experimental results and theoretical predictions for the heavy/light mass ratio. Fig. F1-2 shows the neutron energy spectra in the cm system for the heavy fragment (open circles) and light fragment (closed circles).

The observed angular- and energy-distributions are in agreement with the assumption of isotropic evaporation from fully accelerated fragments; no evidence for pre-equilibrium emission is found. The results indicate that, for the fully relaxed component of the strongly damped collisions, the system is close to thermal equilibrium at the end of the interaction.

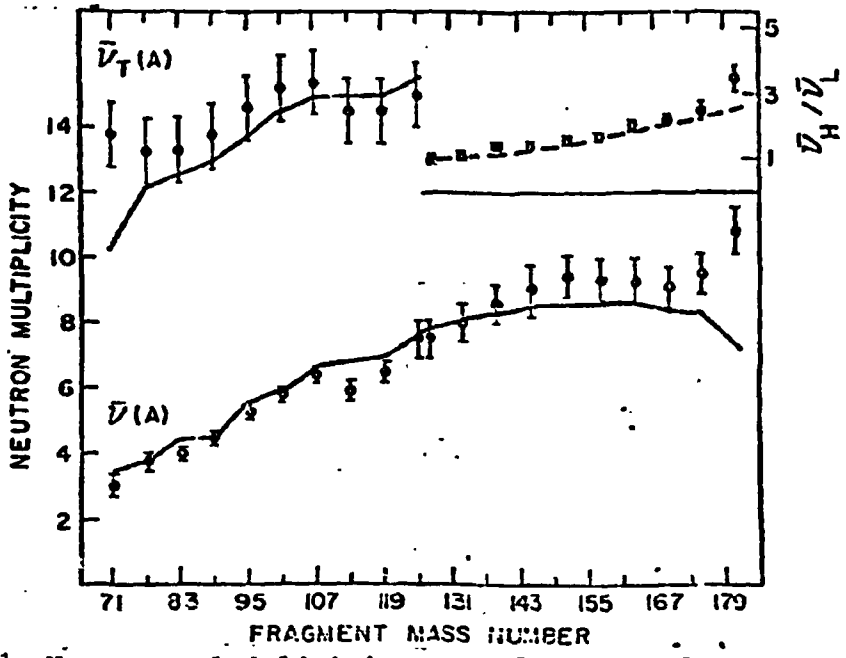

Fig. F1-1 Neutron multiplicities as a function of mass number for collisions between ^{86}Kr and ^{166}Er.

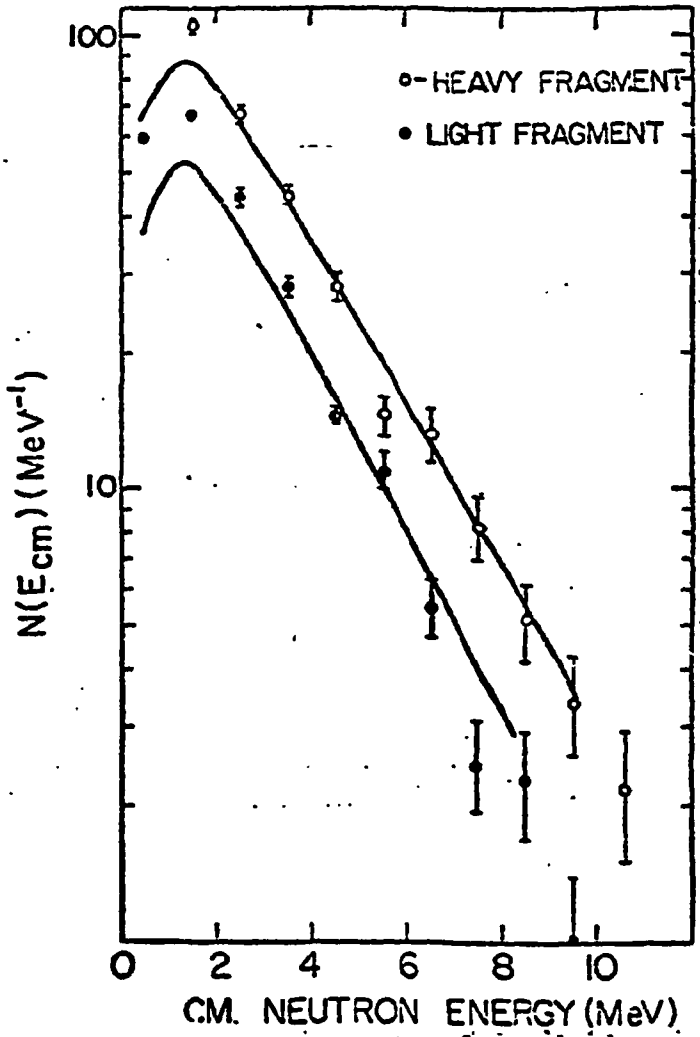

Fig. F1-2 Neutron c.m. energy spectra from the heavy and light fragments, emitted in reactions between ^{86}Kr and ^{166}Er.

G. ACCELERATOR DEVELOPMENT AND INSTRUMENTATION

1. Energy Stabilization of The Tandem Van de Graaff Accelerator for High Resolution Measurements (M.E. Bleck,* E.G. Bilpuch, G.E. Mitchell, W.A. Watson, W.K. Wells,** C.R. Westerfeldt)

Work is proceeding along several avenues to improve the performance and reliability of the high resolution system of the FN tandem Van de Graaff accelerator. This system was described in past reports. Recently a light pipe was fabricated and installed between the low energy baseplate and the terminal to carry the correction signal to the high voltage amplifier. This light pipe replaces a collimated light beam and should reduce the noise in the system due to light scattered off the accelerator rings. A new terminal amplifier with a higher current capacity has been constructed and is presently being bench tested. In addition, two new slit current pre-amplifiers have been constructed with several design changes to reduce noise, and are also being bench tested.

Another major avenue of development concerns the 90-90 analyzing magnet system. Some modifications to the present NMR magnetic field probe (used to "field lock" the magnets) which improve the signal to noise ratio of the detected resonance are being tested. These modifications should allow better control of the magnetic field and hence of the beam energy. Also under investigation is the use of other types of NMR probes. A microprocessor is being built which will step the programming voltage to the magnets on command from the computer; this task is presently handled by the computer itself. This programming voltage, in conjunction with a programmable frequency synthesizer serving as a reference for the NMR fluxmeter, allows the computer to stop the beam energy.

Finally, some testing has been performed (and is continuing) on the use of very thin stripping foils in place of gas stripping. Thus far the results are negative but designs for thinner and more durable foils will be tested in the near future.

H. COMPUTER RELATED DEVELOPMENT

1. The Prime Computer System (J.R. Chandler,* B.H. Chou, K.B. Sales, C.R. Westerfeldt, S.E. Edwards)

During the past 12 months, the PRIME 300 computer system has been improved in several areas. Two BEEHIVE video terminals have been obtained to replace the two teletype terminals. This has greatly speeded up the I-O operations as the video units operate at 2400 BAUD instead of the 110 BAUD of the older teletypes. Secondly, this change has virtually eliminated down time as the result of I-O device failure. To provide hard copy output, we have purchased a DECWRITER III which is capable of output at 2400 BAUD, but is at present limited by software to 300 BAUD continuous output. The DECWRITER may also be substituted for either BEEHIVE terminal in case of failure.

The PRIME 300 computer itself has been upgraded by the addition of a 32K word board. This addition brings up the memory size to 64K words. With the 32K of memory, we were restricted in our data taking program to four charged particle or NaI spectra, plus a GeLi spectra. This had not been a problem in the past, but a new series of experiments required at least five spectra plus a GeLi spectra be stored in order to measure some more complex angular distributions.

With the 64K of memory installed and working, we have brought up the full PRIMOS II REV II operating system. This system has many advantages over the REV 10 system which we had been using. This revision seems to be the best for our single user system, and at this point we do not anticipate upgrading the system to higher revisions.

The new larger memory and operating system have allowed us to adapt several analysis programs from the old DDP-224 computer to the PRIME computer. This decreases our dependence on the DDP-224, and will greatly benefit programmers writing software for the proposed new computer system for the Tandem laboratory.

The CAMAC interface has been expanded with the addition of two quad input - 16 bit scalers, and one dual input - 16 bit preset scaler. The quad scalers will allow the data taking program to read in data such as the live time, total integrated charge, or data from single channel analyzers. The preset scaler will be used to count the integrated charge and initiate a sequence of events when the preset has been reached. This will be of great help in our elastic scattering experiments as it will free the experimenter of several operations previously required when preset was reached on the isolated preset scaler.

---

*Now at Savannah River

M. NUCLEAR THEORY AND PHENOMENOLOGY

1. Many-Body Reaction Theory (S.R. Cotanch)

A simple unitary estimate for multi-step processes has been developed. The results have been recently reported[1] and submitted for publication in Physical Review C. The abstract of the manuscript follows:

> "Utilizing the unitary constraint for an N dimensional S-matrix and phase averaging arguments, a simple expression is derived to provide realistic bounds on the exact multi-step transition rate for the general reaction A(a,b)B. The formula, which approximately includes a large class of multi-step processes, is designed for practical upper estimates of cross section variation due to higher-order contributions from N reaction channels. The result establishes model-inaependent guidelines for the importance of higher-order effects and represents a "sum rule" for multi-step phenomena. Applications to the reactions $^{208}Pb(p,t)^{206}Pb(3^+)$ and $^{48}Ca(^{16}O,^{15}C)^{49}Ti$ which are improbable or forbidden in the one-step DWBA, yields cross section estimates that are within an order of magnitude agreement with observation."

---

[1] S.R. Cotanch, B.A.P.S. 23, 931 (1978)

2. Computer Code Development for Particle Capture and Polarized Charge Exchange Reactions (S.R. Cotanch)

The code RADCAP, which computes direct radiative particle capture processes, has been generalized to a coupled channels capture code (EXCAP) by including the isobaric analogue of the target nucleus. EXCAP now requires input specification of both proton and neutron effective charges as well as parameters for the Lane potential which governs the coupling between target and analogue. Further physical details can be found elsewhere.[1]

The code TWAVE, which computes charge exchange reactions, has also been generalized (TWAVE2) to compute analyzing powers. In addition an isovector spin-orbit interaction $(\vec{l}\cdot\vec{s})\,(t\cdot T)$ term has been included. The physical significance of this operator has been recently investigated in a phenomenological analysis[2]. (See Section I-5.)

These codes have been made available to all TUNL personnel.

3. Kaon-Nucleus Studies (S.R. Cotanch)

Investigations concerning the feasibility of using the K^+ meson (kaon) as a nuclear structure probe have continued. The major results obtained have been reported and have been accepted for publication.[4,5] The respective abstracts follow:

> "The plane wave impulse approximation (PWIA) is assessed for K^+ meson inelastic scattering from ^{16}O by comparison with distorted wave impulse approximation (DWIA) calculations. The K^+-nucleus distortions are directly determined from phenomenological K^+-nucleon amplitudes. For $E_{Lab} \geq 50$ MeV use of plane waves enhances the DWIA cross section less than 50%, an effect size comparable to distorted wave calculations with different sets of K^+-nucleon amplitudes."

> "K^+ meson (kaon) inelastic excitation of low-lying ($E_x = 0 - 15$ MeV) $T = 0$ collective states in ^{16}O is theoretically studied as a function of energy and momentum transfer. The distorted wave impulse approximation is used to calculate angular distributions and total inelastic cross sections for exciting the first $J^\pi = 2^+, 3^-, 4^+$, and 5^- states at lab energies from threshold to 400 MeV. The distortions are represented in a Kisslinger-type optical potential constructed from elementary K^+-nucleon amplitudes. Total nuclear elastic and reaction K^+-nucleus cross sections are computed to demonstrate sensitivity to choice in K^+-nucleon amplitudes. Fermi motion effects are also assessed using a simple averaging

[1] S.R. Cotanch, Phys. Lett. 76B, 19 (1978)
[2] R.C. Byrd, R.L. Walter, S.R. Cotanch, submitted to Phys. Rev. Lett.
[3] S.R. Cotanch, B.A.P.S. 23, 554 (1978)
[4] S.R. Cotanch, Phys. Rev. C18 (October, in press)
[5] S.R. Cotanch, Nucl. Phys. A (in press, late 1978 or early 1979)

procedure. The weak absorption character of the kaon is reflected in the inelastic calculations which predict selective excitation of low spin states at low momentum transfer and high spin states at high momentum transfer."

4. Test of Nuclear Structure Models (S.R. Cotanch, J.M. Lafferty)

Progress is continuing in the study of nuclear clustering (correlations) using a simple few-cluster model.[1] The cluster effective two-body interaction is adjusted[1] such that the important static observed nuclear properties are reproduced. Of current interest are the continuum states above the particle emission threshold. These states are being investigated through particle capture processes. The capture code RADCAP has been modified to include the cluster interaction for both the bound state and the continuum and calculations are presently being performed for the specific reaction (α,γ) on a number of light nuclei. The results of these calculations should not only have ramifications in the area of cluster transfer reactions but also, and perhaps more importantly, should provide new information concerning isoscalar giant resonances. Much of this work will be included in Lafferty's Ph.D. dissertation.

---

[1] B.Buck and A.A. Pilt, Nucl. Phys. A295, 1 (1978); A280, 133 (1977)

5. Consistent Lane Model Analyses of The Complete ^{9}Be + Nucleon Data Set

(R.C. Byrd, R.L. Walter, S.R. Cotanch)

It has long been recognized that global optical model systematics suggest a symmetry dependence in the neutron and proton potentials. This implicit relationship is formally expressed in the Lane model, which further predicts isospin coupling to the quasi-elastic (p,n) reaction. This model forms the basis of subsequent applications of explicit isospin constraints to optical model analyses which include the (p,n) channel. Although it is clear from these analyses and global symmetry-dependent elastic models that the Lane assumptions are generally valid, the conclusions have been inconsistent in approach and limited in scope. As a result, no definitive test exists of the Lane model's ability to predict a complete set of observables for (p,p), (p,n), and (n,n) reactions with a single consistent potential. It is therefore not known whether the isospin constraints will allow description of such a full data set with agreement comparable to that of single-channel analyses. Such a determination is the immediate goal of our Lane model program, and we feel that our success shows the elegance that the constrained, coupled approach brings to the optical model.

We divide this report into two sections, the first of which includes the results reported last year. Its basic assumption, guided by Hartree-Fock calculations, is that the symmetry potential for light nuclei such as ^{9}Be should be broadly surface-peaked. Our initial results were that such a potential allows an excellent description of most of the ^{9}Be + nucleon data over the 11 to 15 MeV energy range. Specifically, the (p,p), (n,n), and (p,n) cross sections σ_{pp}, σ_{nn}, and σ_{pn} and the (p,p) analyzing powers A_{pp} are well represented. However, no simultaneous description of the (p,n) analyzing powers A_{pn} could be found. (Bull. Am. Phys. Soc. 23, 926 (1978).

An intensive effort was made next to explain the A_{pn} results. Reanalysis after we included in the model a symmetry spin-orbit term $V^1_{s.o.}(\vec{l}\cdot\vec{s})(\vec{t}\cdot\vec{T})$ showed that excellent agreement could be obtained for the complete set of observables near 13 MeV, as shown in Fig. I5-1a. It was found, however, that this solution cannot be satisfactorily extended to neighboring energies. Our conclusion concerning the analysis with surface symmetry potentials is that excellent agreement is obtained without the $V^1_{s.o.}$ term for all but the A_{pn} results. Further, addition of this term allows good description of the complete data set (but only at a single energy). Results of these analyses were submitted to Physical Review Letters but have now been held up

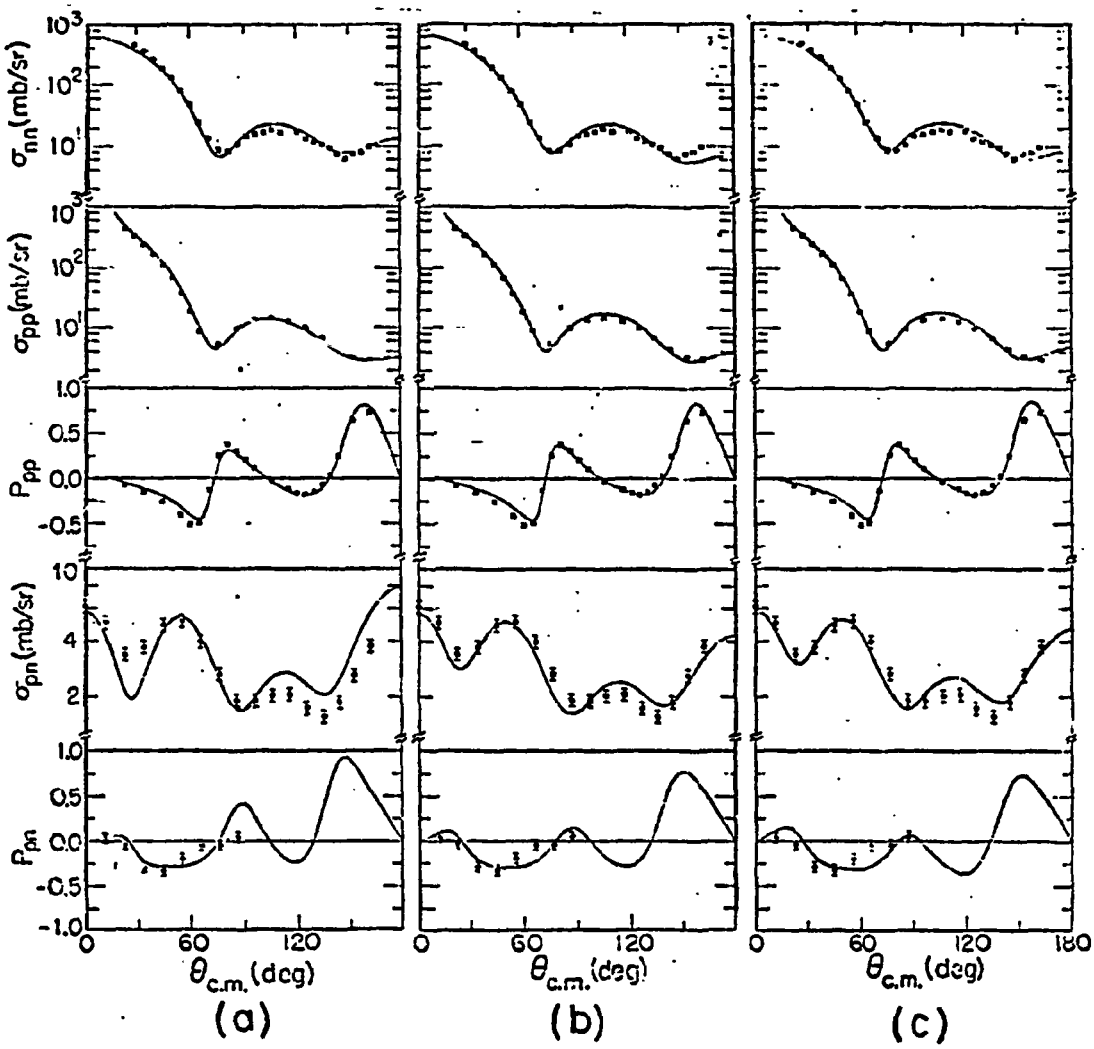

Fig. I5-1 Lane model calculations of ^{9}Be + nucleon results near 13 MeV using different assumptions. (a) Surfaced-peaked real symmetry term with symmetry spin-orbit potential. (b) Volume real symmetry term with symmetry spin-orbit potential. (c) Volume real symmetry term without spin-orbit potential.

by us because of results from a continuation of the analysis as described below.

The second set of analyses were based on a real symmetry potential with a volume shape. We present here two solutions. The first is an optical potential constrained to constant geometries, linearly-varying strengths, and small spin-orbit and Coulomb correction terms. The results, shown in Figure I5-2,

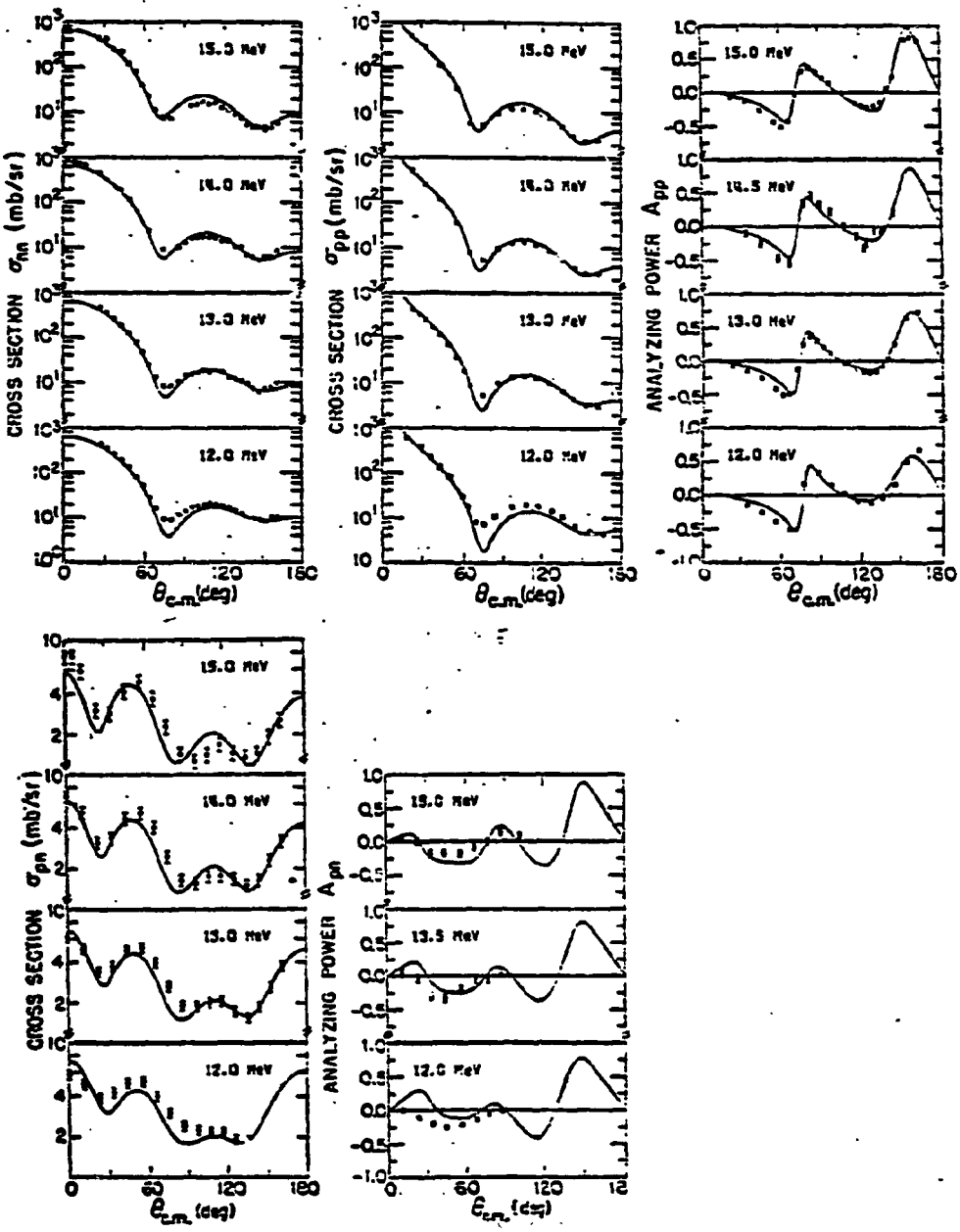

Fig. I5-2 Predictions of observables for the ^{9}Be + nucleon system from 12.0 to 15.0 MeV using a single Lane potential with constant geometries, linearly varying strengths, and a volume real symmetry term.

are a dramatic improvement over the previous surface-peaked solution, both in quality of agreement and energy range of applicability which now extends from 12 to 15 MeV. The second volume analysis used a published energy-dependent optical model for ^{9}Be(p,p) as a starting potential. Within the quality of the overall data set, over the full 8- to 15-MeV range the agreement shown in Fig. I5-3

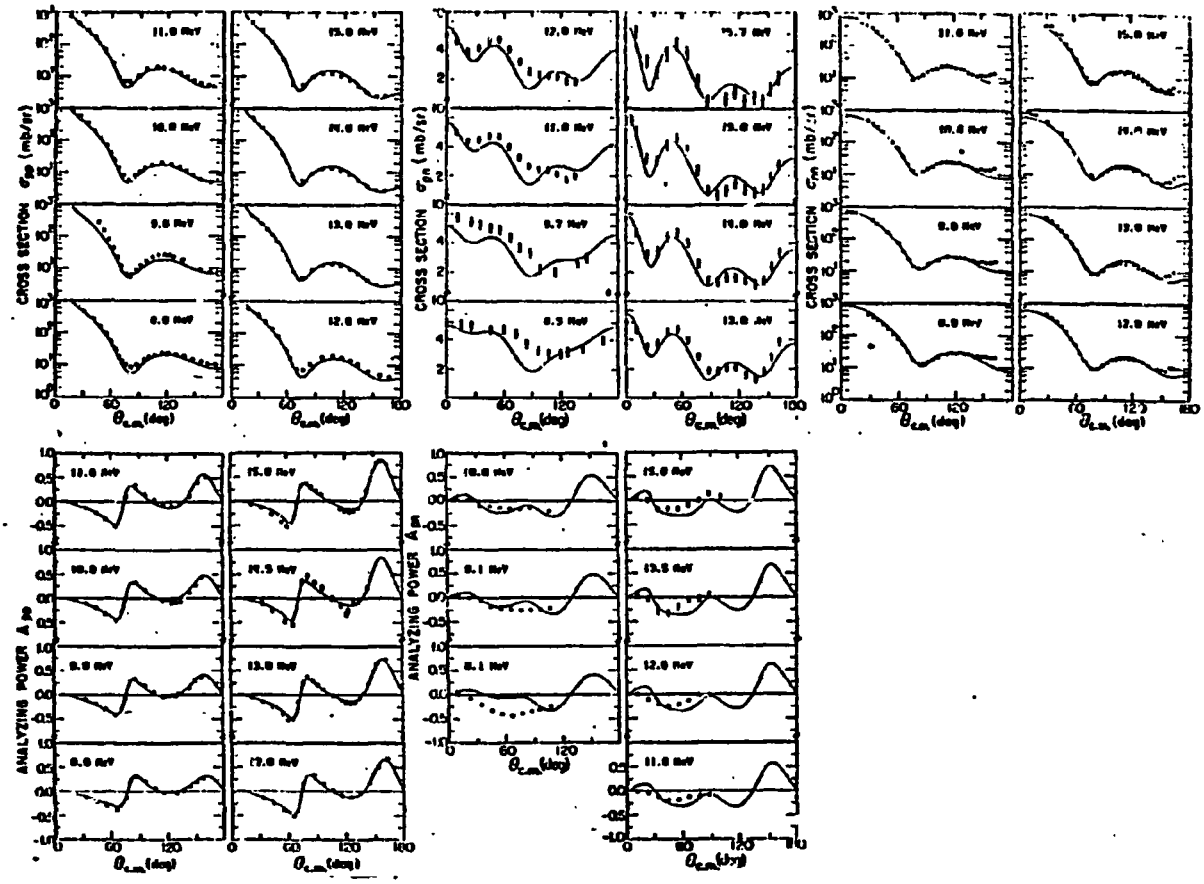

Fig. I5-3 Predictions of observables for the ^{9}Be + nucleon system from 8 to 15 MeV using a single Lane potential with smoothly energy-dependent parameters and a volume real symmetry term.

is indeed comparable to that of single-channel analyses which span a wide energy range.

Our conclusion is thus that the Lane model appears to be as valid as the optical potentials that it connects. These results were presented at the Livermore conference on the optical model and (p,n) reactions and at the 1978 meeting of the American Physical Society Division of Nuclear Physics at Asilomar.

Current analysis is focussed on resolving details of the Lane potentials discussed above. As illustration, Fig. I5-1 shows the best descriptions of the 13-MeV data obtained with three different assumptions. Part (a) shows the prediction using spin-orbit and surface real symmetry potentials. Part (b) gives the similar results with a volume shape, and Part (c) gives the results for a volume shape without spin-orbit $V'_{s.o.}$. Clearly, no unambiguous determination of the necessity of various features can be made, even in our severely constrained analysis. Future studies are anticipated on heavier targets such as the Sn isotopic sequence or the heavy, spherical ^{208}Pb nucleus. Such systems may eliminate some difficulties associated with the highly-deformed ^{9}Be target and answer questions about Coulomb effects which negligible in light nuclei.

6. Dynamical Two-Center Shell Model and Unified Treatment of Heavy-Ion Scattering and Transfer Reactions (J. Y. Park, W. Scheid ((Univ. of Giessen)), W. Greiner ((Univ. of Frankfurt)))

The two-center shell model, which was mostly used for static calculations up to now, has been extended to a dynamical model. Scattering and transfer reactions induced by heavy ions are described in a unified fashion using the dynamical two-center shell model. Molecular wave functions are constructed from the two-center wave functions, taking into account the antisymmetrization of the valence nucleons and symmetrization of the cores. Elastic and Inelastic scattering and one-nucleon transfer reactions are considered in the coupled-channel formalism. The advantage of using the two-center molecular wave functions lies in the fact that already a large fraction of the interaction between the nucleons and the cores is contained in the two-center potential. Polarization or dynamical orientation effects are also included due to the dependence of the molecular wave functions on the relative coordinate. Another advantage of the two-center molecular treatment is that it eliminates the problem of non-orthogonality of the channel bound-state wave functions in the conventional one-center formulations. The present formulation, which includes explicitly the coupling between the direct and transfer channels, is especially convenient to study the effects of transfer channels on the scattering of heavy ion systems and the antisymmetrization effects. A report on this work was given at the International Conference on Nuclear Structure in Tokyo, Japan.

7. Two-Center Level Structure and the Landau-Zener Excitation Mechanism in Heavy Ion Collisions (J.Y. Park, W. Greiner ((Univ. of Frankfurt)), W. Scheid ((Univ. of Giessen)))

According to the Landau-Zener mechanism in atomic collisions, excitations occur mainly in avoided level crossings, causing the system to jump from one energy surface to another. In order to examine the possibility of the Landau-Zener excitation mechanism in asymmetric heavy ion collisions we have calculated single-particle energies as a function of the internuclear separation distance R for several target projectile combinations, such as $^{13}C + ^{16}O$, $^{12}C + ^{17}O$, $^{9}Be + ^{16}O$ and $^{8}Be + ^{17}O$. The asymmetric two-center shell model which includes $\vec{l} \cdot \vec{s}$ and l^2 terms is used to calculate the single particle energies. The parameters of the two-center potential are determined by fitting the experimental level structure near the Fermi levels of the separated nuclei ($R \to \infty$) and the corresponding compound nucleus ($R \to 0$). Our calculations suggest that the cross sections for the excitation and transfer of nucleons in these reactions should exhibit certain enhancements as function of the heavy ion energies which arise due to avoided level crossings in the two-center energy level diagrams. It would be a unique signature for the formation of nuclear molecular orbits if the promotion process for nucleons could be detected in the excitation and transfer cross sections. Such experiments, which can give an answer to the important problem of the existence of molecular orbits in nuclear heavy ion collisions, are proposed. A report on this work was given at the American Physical Society meeting

in Washington.

8. Quasimolecular States in the $^{12}C - ^{12}C$ System (J.Y. Park, W. Greiner ((Univ. of Frankfurt)), W. Scheid ((Univ. of Giessen)))

Structure of non-statistical origin in the $^{12}C - ^{12}C$ cross section near the Coulomb barrier has been interpreted as quasimolecular resonances. We have applied the molecular-type adiabatic potential, which reproduced the position and the spacing of the observed sub-coulomb resonances well,[1] for the explanation of the resonances above the Coulomb-barrier up to $E_{C.M.} = 14$ MeV. We have coupled the first excited 2^+-state on the elastic channel and obtained intermediate structures in the cross sections at energies at wnich the conditions for the double resonance effect are fulfilled. The effects of the coupling on the reflection and transition coefficients are studied systematically. The abstract of this work, published in Physical Review, is:

> "Quasimolecular resonance structures in the ^{12}C-^{12}C system are studied in the framework of the coupled channel formalism in the energy range $E_{C.M.} = 5$–14 MeV. The influence of the coupling of the first excited 2^+ state in ^{12}C on the resonance structures is investigated by choosing various types of coupling potentials. The intermediate structures in the reflection and transition coefficients and cross sections can be interpreted with the double resonance mechanism."

A review of this topic was given as an invited talk at the Iowa Workshop on Double Folding Potentials for Heavy Ion Interactions, March 31-April 1, 1978.

9. Application of The Dynamical Two-Center Shell Model to the $^{13}C + ^{13}C$ Scattering (G. Terecki ((Univ. of Giessen)), W. Scheid ((Univ. of Giessen)), J.Y. Park)

The dynamics of the valence nucleon in the nucleus-nucleus scattering is described by the dynamical two-center shell model with molecular wave functions. The Hamiltonian operator contains the couplings which arise due to the rotation of the molecular coordinate systems (centrifugal and Coriolis terms) and the shift of the nuclear center (radial coupling). The effects of these couplings on the elastic and inelastic scattering of the $^{13}C + ^{13}C$ system are investigated. Further the theory of dynamical two-center shell model has been generalized to treat the neutron transfer and elastic and inelastic scattering in a unified fashion. A report on this work was given at the German Physical Society meeting in Berlin.

---

[1] J.Y. Park et al., Phys. Rev. C10 (1974) 967

10. Helicity Formulation of Collisions for Systems with Channel Spins One and Two (G.J. Grube, J.Y. Park)

Advances in the field of polarized heavy ions have given added importance to the collision problem between particles with spin one or larger spins. Apart from its simple mathematical elegance the helicity formalism is easily adaptable for the scattering problems with arbitrary spin. We have obtained in the helicity formalism explicit expressions for the scattering amplitudes in terms of the phase shifts for systems with channel spin up to two. The expressions involve only a sum over the total angular momentum J, instead of the five sums in the customary formalism. Some recursion formulae for the reduced rotational wave functions which are useful in the applications are also obtained. The present formalism is especially convenient and advantageous for scattering involving a large number of partial waves as in heavy ion scattering at medium and high energies. It can greatly reduce computational efforts to study, for example, the effects of spin dependence in the nucleus-nucleus interaction for scattering of two spin one particles, such as d, ^{6}Li, ^{14}N, ^{32}P as well as scattering of spin 1/2 particles with spin 3/2 particles, such as ^{7}Li, ^{9}Be, ^{11}B and ^{23}Na.

11. Theory of Nucleon Transfer in The Dynamical Two-Center Shell Model (J.Y. Park, W. Scheid ((Univ. of Giessen)), W. Greiner ((Univ. of Frankfurt)))

A paper with the above title has been submitted to Physical Review. The abstract follows:

> "The theory of nucleon transfer in heavy ion reactions is formulated on the basis of the molecular particle-core model for a system consisting of two cores and one extra-nucleon. The extra-nucleon is described by the molecular wave functions of the asymmetric two-center shell model (ATCSM). The cores can be collectively excited and are treated with vibrator-rotator models. The potentials for shape polarization are contained in the ATCSM and the interaction between the cores. The excitation and transfer of the extra-nucleon is induced by the radial and rotational couplings. The coupled channel equations which include the recoil effects in first approximation are derived in a form suitable for numerical calculations of cross sections."

APPENDIX I

A. PUBLISHED TUNL JOURNAL ARTICLES AND ARTICLES BY NCSU-TUNL PERSONNEL

January 1976-December 1978

1. High-Resolution Study of the $^{26}Mg(p,p)$ Reaction. C.R. Westerfeldt, G.E. Mitchell, E.G. Bilpuch, and D.A. Outlaw, Nucl. Phys. A303 (1978) 111.

2. New Probe of Line Broadening with Resolvable Fine Structure: The "Off-Diagonal Strength Function", A.M. Lane, T.R. Dittrich, G.E. Mitchell, and E.G. Bilpuch, Phys. Rev. Letters 41 (1978) 454.

3. Neutron Emission in Strongly Damped Collisions of ^{86}Kr on ^{166}Er at 602 MeV, Y. Eyal, A. Gavron, I. Tserruya, Z. Fraenkel, Y. Eisen, S. Wald, R. Bass, C.R. Gould, G. Kreyling, R. Renfordt, K. Stelzer, R. Zitzmann, A. Gabbi, U. Lynen, H. Stelzer, I. Rode, R. Bock, Phys. Rev. Letters 41 (1978) 625-628.

4. Neutron Multiplicities in Inelastic Collisions of ^{132}Xe with ^{197}Au, C.R. Gould, R. Bass, J.V. Czarnecki, V. Hartmann, K. Stelzer, R. Zitzmann, Y. Eyal, Zeitschrift für Physik A284 (1978) 353-354.

5. Confirmation of 8+ Assignment to the 11.86 MeV Level in ^{24}Mg, S.A. Wender, C.R. Gould, D.R. Tilley, D.G. Rickel, R.W. Zurmühle, Phys. Rev. C17 (1978) 1365-1367.

6. Angular Distribution Measurements for Radiative Capture of Fast Neutrons by ^{40}Ca, H.R. Weller, R.A. Blue, P.L. von Behren, N.R. Roberson, C.R. Gould, D.R. Tilley, S.A. Wender, Phys. Rev. C17 (1978) 1260-1263.

7. Differential Elastic and Inelastic Scattering of 7- to 15-MeV Neutrons from Beryllium, H.H. Hogue, P.L. von Behren, D.H. Epperson, S.G. Glendinning, P.W. Lisowski, C.E. Nelson, H.W. Newson, F.O. Purser, W. Tornow, C.R. Gould, L.W. Seagondollar, Nucl. Science and Engineering 68 (1978) 38-42.

8. Polarized Proton Capture on ^{59}Co, J.D. Turner, C.P. Cameron, H.R. Weller, N.R. Roberson, D.R. Tilley, Phys. Rev. C17 (1978) 1853

9. Polarized Proton Capture in the Giant Dipole Resonance Region, H.R. Weller, N.R. Roberson, and S.R. Cotanch, Phys. Rev. C18 (1978) 65.

10. Quadrupole Radiation in Fast Neutron Capture on ^{40}Ca, S.A. Wender, N.R. Roberson, M. Potokar, H.R. Weller, D.R. Tilley, Phys. Rev. Letters 41 (1978) 1217.

11. Large Charge Exchange Corrections to Direct Photonuclear Processes, S.R. Cotanch, Phys. Lett. 76B (1978) 19.

12. Plane Waves for Kaon-Nucleus Reactions, S.R. Cotanch, Phys. Rev. C18 (1978) 1941.

B. JOURNAL ARTICLES ACCEPTED FOR PUBLICATION

1. Study of Inelastic Proton Amplitudes for a Fragmented Analogue State in ^{45}Sc, G.E. Mitchell, T.R. Dittrich, and E.G. Bilpuch, accepted for publication in Zeitschrift für Physik.

2. Elastic and Inelastic Scattering of 7- to 14- MeV Neutrons from Lithium-6 and Lithium-7, H.H. Hogue, P.C. von Behren, D.W. Glasgow, S.G. Glendinning, P.W. Lisowski, C.E. Nelson, F.O. Purser, W. Tornow, C.R. Gould and L.W. Seagondollar, accepted for publication in Nuclear Science and Engineering.

3. Selective Excitation in Kaon-Nucleus Inelastic Scattering, S.R. Cotanch, accepted for publication in Nucl. Phys. A.

C. JOURNAL ARTICLES SUBMITTED FOR PUBLICATION

1. Measurements of the Reactions $^{15}N(\gamma,d_0)^{13}C$ and $^{13}C(\vec{\gamma},\gamma_0)^{15}N$ in the Giant Resonance Region, D.M. Skopik, J.J. Murphy, H.R. Weller, R.A. Blue, N.R. Roberson, S.A. Wender and D.R. Tilley, submitted to Phys. Rev. C.

2. Detailed Study of the Lane Potential: Multi-Channel and Polarization Constraints, R.C. Byrd, R.L. Walter, and S.R. Cotanch, submitted to Phys. Rev. Letters.

3. Simple Unitary Estimate for Multistep Processes, S.R. Cotanch, submitted to Phys. Rev. C.

APPENDIX II

INVITED TALKS, CONFERENCE AND TECHNICAL REPORTS AND BOOK CHAPTERS BY NCSU-TUNL PERSONNEL

January 1978-December 1978

1. High Resolution Proton Resonance Studies, G.E. Mitchell (invited talk, Small Accelerator Conference) Bull. Am. Phys. Soc. 23 1023 (1978)

2. Experimental Demonstration of Phase Relations for Common Doorway States, G.E. Mitchell, T.R. Dittrich and E.G. Bilpuch, presented at Third International Symposium of Neutron Capture Gamma-Ray Spectroscopy, Brookhaven National Laboratory, Sept. 18-22, 1978, to be published.

3. Evidence for an E2 Resonance Observed by Radiative Capture of Fast Neutrons by ^{40}Ca, N.R. Roberson, M. Potokar, D.R. Tilley, S.A. Wender and H.R. Weller, to be published in "Proceedings of the Third International Symposium on Neutron Capture Gamma-Ray Spectroscopy and Related Topics", Sept. 1978.

4. Extension of the Lane Model to Light Nuclei, Roger C. Byrd, Richard L. Walter, and Stephen R. Cotanch, to be published in Lecture Notes in Physics 84, Springer-Verlag, Heidelberg, ed. by H. Zankel.

APPENDIX III

ABSTRACTS OF CONTRIBUTED PAPERS PRESENTED AT AMERICAN PHYSICAL SOCIETY AND OTHER MEETINGS

1. High Resolution Study of the $^{26}Mg(p,p)$ Reaction, C.R. Westerfeldt, G.E. Mitchell, D.A. Outlaw, and E.G. Bilpuch, Bull. Am. Phys. Soc. 23, 520 (1978).

2. High Resolution Proton Inelastic Scattering on ^{46}Ti, J.R. Chandler, G.E. Mitchell, and E.G. Bilpuch, Bull. Am. Phys. Soc. 23,521 (1978).

3. High Resolution Proton Inelastic Scattering on ^{48}Ti, W.K. Wells, E.G. Bilpuch, and G.E. Mitchell, Bull. Am. Phys. Soc. 23, 521 (1978).

4. A High Resolution Study of the Lowest $1/2^+$ Analogue State in ^{91}Nb, M.E. Bleck, W.K. Wells, D.A. Outlaw, C.R. Westerfeldt, E.G. Bilpuch and G.E. Mitchell, Bull. Am. Phys. Soc. 23, 554 (1978).

5. Angular Distribution Measurements for the $^{40}Ca(n,\gamma_0)^{41}Ca$ Reaction, S.A. Wender, H.R. Weller, D.R. Tilley, N.R. Roberson, M. Potokar, M. Jensen, Bull. Am. Phys. Soc. 23, 507 (1978).

6. Polarized Proton Capture on ^{13}C, J.D. Turner, N.R. Roberson, S.A. Wender, H.R. Weller, D.R. Tilley, Bull. Am. Phys. Soc. 23, 602 (1978).

7. Neutron Multiplicities in Inelastic Collisions of ^{132}Xe with ^{197}Au, C.R. Gould, R.Bass, J.V. Czamecki, V. Hartmann, K. Stelzer, R. Zitzmann, Y. Eyal, Bull. Am. Phys. Soc. 23, 523 (1978).

8. Neutron Scattering from ^{11}B, C.R. Gould, S.G. Glendenning, H.H. Hogue, C.E. Nelson, A. Beyerle, S. El-Kadi, H.W. Newson, F.O. Purser, L.W. Seagondollar, Bull. Am. Phys. Soc. 23, 635 (1978).

9. Lane Model Analysis of (p,p), (p,n_0) and (n,n) Reactions on ^{9}Be, R.C. Byrd, R.L. Walter and S.R. Cotanch, Bull. Am. Phys. Soc. 23, 526 (1978).

10. Evidence for Surface-Peaked Real and Spin-Orbit Symmetry Potentials in the Optical Model, R.C. Byrd, R.L. Walter, and S.R. Cotanch, Bull. Am. Phys. Soc. 23, 926 (1978).

11. Kaon Excitation of High Spin States, S.R. Cotanch, Bull. Am. Phys. Soc. 22, 1021 (1977).

12. Unitary Estimate for Multistep Processes, S.R. Cotanch, Bull. Am. Phys. Soc. 23, (1978).

13. Comparison of Radiative Electron Capture by Cl Ions in C and Cu, S.M. Shafroth, A. Kodre, J.A. Tanis, J. Willis and R. Mowat, Bull. Am. Phys. Soc. 23, 598 (1978).

14. Curved Crystal X-Ray Spectrometer of Target and Projectile Cl K Satellites, J.A. Tanis, J. Willis, A. Kodre, S.M. Shafroth, and R. Mowat, Program, Southeastern Section of the American Physical Society, 26-28 Oct. 1978, p22.

APPENDIX IV

REPRINTS OF MATERIAL NOT PREVIOUSLY SUBMITTED

1. High-Resolution Study of the $^{26}Mg(p,p)$ Reaction, C.R. Westerfeldt, G.E. Mitchell, E.G. Bilpuch, and D.A. Outlaw, Nucl. Phys. A303 (1978) 111.

2. New Probe of Line Broadening with Resolvable Fine Structure: The "Off-Diagonal Strength Function", A.M. Lane, T.R. Dittrich, G.E. Mitchell, and E.G. Bilpuch, Phys. Rev. Letters 41 (1978) 454

3. Confirmation of 8^+ Assignment to the 11.86 MeV Level in ^{24}Mg, S.A. Wender, C.R. Gould, D.R. Tilley, D.G. Rickel, R.W. Zurmühle, Phys. Rev. C17 (1978) 1365-1367.

4. Angular Distribution Measurements for Radiative Capture of Fast Neutrons by ^{40}Ca, H.R. Weller, R.A. Blue, P.L. von Behren, N.R. Roberson, C.R. Gould, D.R. Tilley, S.A. Wender, Phys. Rev. C17 (1978) 1260-1263.

5. Differential Elastic and Inelastic Scattering of 7- to 15-MeV Neutrons from Beryllium, H.H. Hogue, P.L. von Behren, D.H. Epperson, S.G. Clendenning, P.W. Lisowski, C.E. Nelson, H.W. Newson, F.O. Purser, W. Tornow, C.R. Gould, L.W. Seagondollar, Nucl. Science and Engineering 68 (1978) 38-42.

6. Polarized Protor Capture on ^{59}Co, J.D. Turner, C.P. Cameron, H.R. Weller, N.R. Roberson, and D.R. Tilley, Phys. Rev. C17 (1978) 1853.

7. Polarized Proton Capture in the Giant Dipole Resonance Region, H.R. Weller, N.R. Roberson, and S.R. Cotanch, Phys. Rev. C18 (1978) 65.

8. Quadrupole Radiation in Fast-Neutron Capture on ^{40}Ca, S.A. Wender, N.R. Roberson, M. Potokar, H.R. Weller, D.R. Tilley, Phys. Rev. Letters 41 (1978) 1217

9. Large Charge Exchange Corrections to Direct Photonuclear Processes, S.R. Cotanch, Phys. Lett. 76B (1978) 19.

Reprints Removed